[Article] A local-in-space-timestep approach to a finite element discretization of the heat equation with a posteriori estimates

SIAM J. NUMER. ANAL.
Vol. 47, No. 4, pp. 3109–3138

A LOCAL-IN-SPACE-TIMESTEP APPROACH TO A FINITE ELEMENT DISCRETIZATION OF THE HEAT EQUATION WITH A POSTERIORI ESTIMATES*

STEFANO BERRONE†

Abstract. A new numerical method is presented for the heat equation with discontinuous coefficients based on a Crank–Nicolson scheme and a conforming finite element space discretization. In the proposed method each node of the spatial discretization may have the global timestep split into an arbitrary number of local substeps in order to pursue a local improvement of the time discretization in the regions of the spatial domain where the solution changes rapidly. This method can possibly be used together with adaptive strategies for both the space discretization and the choice of timesteps to suitably produce an efficient space-time discretizaton of the problem. Robust a posteriori upper and lower bounds of the error are proposed to attain this target. Moreover, some indications are given on how to modify the mesh, the timestep, and the number of substeps to improve the discretization.

Key words. a posteriori error estimates, parabolic problems, multiscale problems, local timesteps, space and time adaptivity

AMS subject classifications. 65N30, 65N15, 65N50, 65J15

DOI. 10.1137/080737058

1. Introduction.

Accurate solutions of problems governed by partial differential equations are required in many practical applications. Adaptive strategies play a key role in obtaining reliable and efficient solutions with reduced computational effort. Many adaptive strategies have been proposed in the last few decades and have been successfully applied to several engineering problems. In the steady elliptic case many questions have received a definitive answer: robust *a posteriori* estimators and convergent and optimal adaptive algorithms are known; see, for example, [2, 3, 7, 10, 13, 16, 17, 19].

Many results regarding error estimators and convergent algorithms [1, 4, 6, 12, 15, 18] are available for the unsteady parabolic case, too, although theory and applications have often been less assessed.

In this work we present a new algorithm based on a conforming finite element discretization in space and a Crank–Nicolson scheme in time. The time discretization is accomplished by combining a global macro timestep (a large timestep common for all the elements of the space discretization) with local substeps (small timesteps different for each element). In this approach, each node of the space discretization may have the global timestep split into an arbitrary number of local substeps.

This approach has been designed to increase the efficiency of an adaptive discretization method in space and in time, and is particularly suitable for all those problems with a solution that displays fast changes in a very small part of the domain and slow changes in most of the spatial domain. In these situations, the fast

*Received by the editors January 2, 2008; accepted for publication (in revised form) July 16, 2009; published electronically September 25, 2009. This work was supported by Italian funds from MIUR-PRIN-2006 "Nuove tecniche di accoppiamento di modelli e di metodi numerici nel trattamento di problemi differenziali," coordinated by Professor Franco Brezzi and by Regione Piemonte via the project "AirToLyMi": "Modeling and simulating sustainable mobility strategies. A study of three real test cases: Turin, Lyon, Milan" (CIPE grant 2006).
http://www.siam.org/journals/sinum/47-4/73705.html

†Dipartimento di Matematica, Politecnico di Torino, Corso Duca degli Abruzzi 24, I-10129 Torino, Italy (sberrone@calvino.polito.it).

changes of the solution would require very small timesteps, but the solution changes very slowly in most of the domain, where the small timesteps are not required and could even compromise efficiency. For these reasons, we propose a method that allows long timesteps for the elements in the regions with slow changes of the solution and small timesteps for the elements in the regions with fast changes. Some numerical experiments are also provided to show that this approach can be effective and efficient in the described situations.

For this method, robust upper and lower residual-type a posteriori error estimates for the error are proved.

The paper is organized as follows. In section 2 the new method is derived and existence, uniqueness, and stability results for the numerical solution are stated. Moreover, a simple numerical test shows good performance of the new method. In section 3 a posteriori upper and lower residual-based estimates for the error are derived and briefly discussed. In section 4 some preliminary numerical investigations on the a posteriori error estimates are presented.

2. Description of the method.

2.1. The continuous problem. Let Ω be a polygonal domain in $\mathbb{R}^d$ with boundary $\partial\Omega$ and let $(0,\Xi)$ be the time interval of interest. We want to find $u : \Omega \times (0,\Xi) \to \mathbb{R}$ such that

$$\frac{\partial u}{\partial t} - \nabla \cdot (\kappa \nabla u) = f \qquad \text{in } \Omega \times (0,\Xi), \tag{2.1}$$

$$u(x,t) = 0 \qquad \text{on } \partial\Omega \times (0,\Xi), \tag{2.2}$$

$$u(x,0) = u^0(x) \qquad \text{in } \Omega \tag{2.3}$$

for any $f \in \mathrm{L}^2(\,(0,\Xi)\,;\mathrm{L}^2(\Omega)\,)$ and $u^0 \in \mathrm{L}^2(\Omega)$. The diffusivity parameter $\kappa(x)$, $0 < \kappa_{min} \le \kappa \le \kappa_{max} < \infty$ is a function that is constant in time and piecewise constant on the polygonal subdomains Ω_d, $d = 1,\dots,D$, with $\cup_{d=1}^{D} \overline{\Omega}_d = \overline{\Omega}$ and $\Omega_i \cap \Omega_j = \emptyset \ \forall i \neq j$.

Setting $W = \left\{ w \in \mathrm{L}^2(\,(0,\Xi)\,;\mathrm{H}^1_0(\Omega)\,) : \frac{\partial w}{\partial t} \in \mathrm{L}^2(\,(0,\Xi)\,;\mathrm{H}^{-1}(\Omega)\,) \right\}$, the variational formulation of the above problem is: *Find* $u \in W$ *such that* $u(.,0) = u^0$ *and*

$$\left\langle \frac{\partial u}{\partial t}, v \right\rangle + (\kappa \nabla u, \nabla v) = (f, v) \quad \forall v \in \mathrm{H}^1_0(\Omega) \ \text{ a.e. in } (0,\Xi)\,. \tag{2.4}$$

Here $\langle\,.\,,\,.\,\rangle$ stands for the duality pairing between $\mathrm{H}^{-1}(\Omega)$ and $\mathrm{H}^1_0(\Omega)$, while $(\,.\,,\,.\,)$ is the usual inner product in $\mathrm{L}^2(\Omega)$. If $u \in W$, then $u \in \mathcal{C}^0([0,\Xi];\mathrm{L}^2(\Omega)\,)$ and the initial condition $u(.,0) = u^0$ is meaningful in $\mathrm{L}^2(\Omega)$.

2.2. The classical numerical discretization. Let us consider a partition of $(0,\Xi)$ into intervals $\left(t^{n-1}, t^n\right)$ of length $\Delta t^n = t^n - t^{n-1}$, with $0 = t^0 < t^1 < \cdots < t^N = \Xi$; let us also set $I^n = \left[t^{n-1}, t^n\right]$. In each timeslab $\Omega \times I^n$, $n \ge 1$, we consider a regular family of partitions $\mathcal{T}_h^n$ of $\overline{\Omega}$ into elements $T \in \mathcal{T}_h^n$, which satisfy the usual conformity and minimal-angle conditions [8]. We denote the diameter of each element $T \in \mathcal{T}_h^n$ by h_T^n and the maximum of h_T^n over all the elements $T \in \mathcal{T}_h^n$ by h^n. From now on the subscript h stands for h^n. We assume that each partition $\mathcal{T}_h^n$ induces partitions of the subdomains Ω_d, $d = 1,\dots,D$ denoted by $\mathcal{T}_{h,d}^n$, so that $\mathcal{T}_h^n = \cup_{d=1}^{D} \mathcal{T}_{h,d}^n$. Let $\mathrm{V}_h^n = \left\{ v_h \in \mathrm{H}^1_0(\Omega) \cap \mathcal{C}^0(\overline{\Omega}) : \ v_{|_T} \in \mathbb{P}_k(T) \ \forall T \in \mathcal{T}_h^n \right\} \subset \mathrm{V} = \mathrm{H}^1_0(\Omega)$ be a family of conforming finite element spaces based on the partitions $\mathcal{T}_h^n$. We denote the space of polynomials of degree $k \ge 1$ on the element $T \in \mathcal{T}_h^n$ by $\mathbb{P}_k(T)$. Assuming $u^0 \in \mathrm{L}^2(\Omega)$,

we define $u^0_{h,\Delta t} = P^1_{h,k}\, u^0$ as the $\mathrm{L}^2(\Omega)$-projection of u^0 on the finite element space V^1_h, and if $u^0 \in \mathcal{C}^0(\overline{\Omega})$, instead of the projection operator $P^1_{h,k}$, we can use an interpolation operator $\pi^1_{h,k} : \mathcal{C}^0(\overline{\Omega}) \to \mathrm{V}^1_h$. Let us introduce the discretization based on the classical Crank–Nicolson scheme for the time integration, using the subscript $h, \Delta t$ to refer to the full discretization in space and in time: $\forall n = 1, \ldots, N$ *find* $u^n_{h,\Delta t} \in \mathrm{V}^n_h$ *such that*

$$\begin{aligned}\left(\frac{u^n_{h,\Delta t} - u^{n-1}_{h,\Delta t}}{t^n - t^{n-1}}, v_h\right) + \frac{1}{2}\left(\kappa \nabla u^n_{h,\Delta t}, \nabla v_h\right) + \frac{1}{2}\left(\kappa \nabla u^{n-1}_{h,\Delta t}, \nabla v_h\right)\\ = \frac{1}{2}\left(\Pi^n_h f^n, v_h\right) + \frac{1}{2}\left(\Pi^n_h f^{n-1}, v_h\right) \qquad \forall v_h \in \mathrm{V}^n_h\,. \end{aligned} \tag{2.5}$$

In the last scalar products of the previous equation we assume that $f \in \mathcal{C}^0([0, \Xi]; \mathrm{L}^2(\Omega))$ and we set $f^r = f(., t^r)$, $r \in \{n-1, n\}$. Moreover, we introduce an arbitrary piecewise polynomial approximation $\Pi^n_h f = \sum_{T \in \mathcal{T}^n_h} \Pi_T f$ of the data f on the elements of the partition $\mathcal{T}^n_h$.

The solution to (2.5) is a continuous, piecewise affine in time approximation of $u(x,t)$ defined $\forall n = 1, \ldots, N$ as

$$u_{h,\Delta t}(x,t) = \frac{t^n - t}{t^n - t^{n-1}}\, u^{n-1}_{h,\Delta t}(x) + \frac{t - t^{n-1}}{t^n - t^{n-1}}\, u^n_{h,\Delta t}(x), \qquad (x,t) \in \Omega \times I^n. \tag{2.6}$$

The solution $u_{h,\Delta t}(x,t)$ is the sum of two terms. The first is the extension to the current timestep of the solution at the end of the previous timestep, and is linearly decreasing to 0 while t approaches t^n. The second is the computed solution at the end of the current timestep times a linear function growing from 0 to 1 in the timestep.

2.3. The new locally substepped trapezoidal method. In this section, we introduce an extension of the previous trapezoidal method. We will refer to this new method as *locally substepped method*. Let us define $\mathcal{N}^n_h$ as the set of all the nodes of a Lagrange basis of V^n_h defined on the partition $\mathcal{T}^n_h$, and for any given set $\omega \subseteq \Omega$, let $\mathcal{N}^n_h(\omega)$ denote the subset of the nodes contained in ω. For each $p \in \mathcal{N}^n_h$, we denote by $\varphi^n_p(x)$ the corresponding Lagrange basis function and we introduce an integer $J^n_p \geq 0$ called *time substep-level*. We assume that adjacent nodes have a bounded jump of the substep-levels.

We are looking for a method in which the solution at the node $p \in \mathcal{N}^n_h$ is continuous, piecewise linear in time over the interval I^n. For each node $p \in \mathcal{N}^n_h$ we consider the interval I^n partitioned into subintervals by the nodes

$$t^{n,k_p} = t^{n-1} + k_p \frac{\Delta\, t^n}{2^{J^n_p}}, \quad k_p = 0, \ldots, 2^{J^n_p}. \tag{2.7}$$

In an adaptive method, when we consider a change of mesh between the $(n-1)$th timeslab and the nth one, the initial condition of the current timeslab is given on the nodes of the partition $\mathcal{T}^{n-1}_h$, whereas all the unknowns of the current timeslab correspond to the nodes of the current mesh $\mathcal{T}^n_h$. To deal with this situation, we define a partition $\mathcal{T}^{n-1,n}_h$, which is a common refinement of the partitions $\mathcal{T}^{n-1}_h$ and $\mathcal{T}^n_h$ [18], and we also define the set $\mathcal{N}^{n-1,n}_h$ as the set of all the nodes of a Lagrange basis of $\mathrm{V}^{n-1,n}_h$ defined on the partition $\mathcal{T}^{n-1,n}_h$. Let us name the Lagrange basis functions of $\mathrm{V}^{n-1,n}_h$ as $\varphi^{n-1,n}_p(x)$. Our solution $\forall x \in \Omega$, $\forall t \in I^n$, $\forall n = 1, \ldots, N$ can be written as follows:

$$u_{h,\Delta t}(x,t) = \mu^n_{h,\Delta t}(x,t) + \nu_{h,\Delta t}(x,t). \tag{2.8}$$

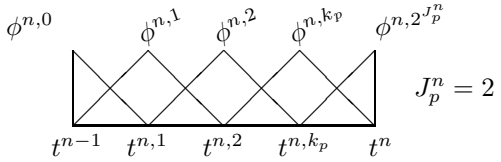

FIG. 1. *Basis functions* ϕ^{n,k_p}.

The function $\mu^n_{h,\Delta t}$ represents the extension to the nth timeslab of the solution at the end of the previous timeslab $u_{h,\Delta t}(x,t^{n-1})$. Here $u_{h,\Delta t}(x,t^{n-1}) \in \mathrm{V}_h^{n-1} \subset \mathrm{V}_h^{n-1,n}$ is interpolated on the nodes $p \in \mathcal{N}_h^{n-1,n}$ of the partition $\mathcal{T}_h^{n-1,n}$. The function $\nu_{h,\Delta t}$ is the computed part of the solution $u_{h,\Delta t}$ in the current timeslab which satisfies $\nu_{h,\Delta t}(x,t^{n-1}) = 0 \ \forall x \in \Omega$.

When coarsening is allowed, in order to define the function $\mu^n_{h,\Delta t}(x,t)$ we need to introduce a time substep-level for the nth timeslab also for the removed nodes. In order to make the method easier to code when a node $p_r \in \mathcal{N}_h^{n-1} \setminus \mathcal{N}_h^n$ is removed, we suggest adding a constraint in the choice of the substep-level of the neighboring nodes. Let us define

$$\mathcal{N}^n_{h,p_r} = \left\{ p \in \mathcal{N}_h^n \ : \ \operatorname{supp} \varphi_p^n \cap \operatorname{supp} \varphi_{p_r}^{n-1,n} \neq \emptyset \right\}.$$

After having chosen the preliminary level J_p^n for each node $p \in \mathcal{N}^n_{h,p_r}$, we define $\hat{J}^n_{p_r} = \max_{p \in \mathcal{N}^n_{h,p_r}} J_p^n$. Then, we set the level $J^{n-1,n}_{p_r}$ of the removed node $p_r \in \mathcal{N}_h^{n-1} \setminus \mathcal{N}_h^n$ equal to $\hat{J}^n_{p_r}$ and we also reassign the level of all $p \in \mathcal{N}^n_{h,p_r}$ equal to $\hat{J}^n_{p_r}$. The effect of this constraint is a local additional refinement of the substep-levels of some nodes, but this can make the coding much simpler and efficient.

We define the time basis functions $\phi^{n,k_p}(t)$, $k_p = 0, \ldots, 2^{J_p^n}$ as the classical Lagrange piecewise linear functions with support in I^n; see Figure 1.

Finally, the functions $\mu^n_{h,\Delta t}(x,t)$ and $\nu_{h,\Delta t}(x,t)$ in (2.8) can be written as follows:

$$\mu^n_{h,\Delta t}(x,t) = \sum_{p \in \mathcal{N}_h^{n-1,n}} u_p^{n-1,n,0} \, \phi^{n,0}(t) \, \varphi_p^{n-1,n}(x),$$

$$\nu_{h,\Delta t}(x,t) = \sum_{p \in \mathcal{N}_h^n} \sum_{k_p=1}^{2^{J_p^n}} u_p^{n,k_p} \, \phi^{n,k_p}(t) \, \varphi_p^n(x),$$

where the coefficients $u_p^{n-1,n,0}$ are obtained by interpolation of the solution at the end of the previous timeslab on the nodes of $\mathcal{N}_h^{n-1,n}$, whereas the coefficients u_p^{n,k_p} are the unknown values of the current timeslab.

Let us define the following space:

$$\mathcal{V}^n_{h,\Delta t} = \operatorname{span} \left\{ \varphi_p^n(x) \times \phi^{n,k_p}(t) : p \in \mathcal{N}_h^n, k_p = 1, \ldots, 2^{J_p^n} \right\}, \tag{2.9}$$

which will be the space containing the unknown function $\nu_{h,\Delta t}$, and let

$$\mathrm{U}^n_{h,\Delta t} = \mu^n_{h,\Delta t} + \mathcal{V}^n_{h,\Delta t} \tag{2.10}$$

contain the whole solution for the nth timeslab.

In order to introduce the method, let us define the characteristic functions $\chi_{k_p}(t)$ of the subinterval $[t^{n,k_p-1}, t^{n,k_p}]$. The space of our test functions W_h^n is the set of

the tensor products of each basis function $\varphi_p^n(x)$ and all the characteristic functions $\chi_{k_p}(t)$, $k_p = 1, \ldots, 2^{J_p^n}$ of the subintervals of the nodes $p \in \mathcal{N}_h^n$ in the nth timeslab:

$$\mathrm{W}_h^n = \operatorname{span}\left\{\varphi_p^n(x) \times \chi_{k_p}(t) \ : \ p \in \mathcal{N}_h^n, k_p = 1, \ldots, 2^{J_p^n}\right\}.$$

For each element $T \in \mathcal{T}_h^n$, we define a substep-level J_T^n as the maximum of the substep-levels of the nodes $p \in \mathcal{N}_h^n(T)$:

$$J_T^n = \max_{p \in \mathcal{N}_h^n(T)} J_p^n \,. \tag{2.11}$$

We also define the following approximate right-hand-side on $\mathcal{T}_h^n \times I^n$:

$$f_{h,\Delta t}(x,t) = \sum_{T \in \mathcal{T}_h^n} \sum_{k_T=0}^{2^{J_T^n}} \Pi_T f(x, t^{n,k_T})\, \phi^{n,k_T}(t). \tag{2.12}$$

The substepped method reads as follows: *For each* $n = 1, \ldots, N$, *find* $u_{h,\Delta t} \in \mathrm{U}_{h,\Delta t}^n$ *such that*

$$\int_{t^{n-1}}^{t^n} \left(\frac{\partial\, u_{h,\Delta t}}{\partial t}, w_h\right) \mathrm{d}t + \int_{t^{n-1}}^{t^n} (\kappa \nabla\, u_{h,\Delta t}, \nabla w_h) \mathrm{d}t = \int_{t^{n-1}}^{t^n} (f_{h,\Delta t}, w_h) \mathrm{d}t \tag{2.13}$$

holds true $\forall w_h \in \mathrm{W}_h^n$.

The method can be rewritten as follows: *For each* $n = 1, \ldots, N$, *find* $u_{h,\Delta t} \in \mathrm{U}_{h,\Delta t}^n$ *such that*

$$\begin{aligned} &\sum_{T \in \mathcal{T}_h^n} \sum_{k_T=1}^{2^{J_T^n}} \int_{t^{n,k_T-1}}^{t^{n,k_T}} \left(\frac{\partial\, u_{h,\Delta t}}{\partial t}, w_h\right)_T \mathrm{d}t + \sum_{T \in \mathcal{T}_h^n} \sum_{k_T=1}^{2^{J_T^n}} \int_{t^{n,k_T-1}}^{t^{n,k_T}} (\kappa \nabla\, u_{h,\Delta t}, \nabla w_h)_T \mathrm{d}t \\ &\qquad = \sum_{T \in \mathcal{T}_h^n} \sum_{k_T=1}^{2^{J_T^n}} \int_{t^{n,k_T-1}}^{t^{n,k_T}} (f_{h,\Delta t}, w_h)_T \mathrm{d}t \end{aligned} \tag{2.14}$$

holds true $\forall w_h \in \mathrm{W}_h^n$.

Remark 2.1. In some element $T \in \mathcal{T}_h^n$ we have nodes $p \in \mathcal{N}_h^n(T)$ with level $J_p^n < J_T^n$. Some values of $u_{h,\Delta t}(x_p, t^{n,k_T})$ that do not correspond to the unknown values in (2.8) are involved in assembling the linear system (2.14). As the solution $u_{h,\Delta t}$ is piecewise affine in time in each point, these quantities can be expressed as weighted combinations of the unknown values u_p^{n,k_p}, and these values are treated as hanging nodes in the time discretization:

$$u_{h,\Delta t}(x_p, t^{n,k_T}) = \left(1 - \frac{\operatorname{mod}(k_T, 2^{J_T^n - J_p^n})}{2^{J_T^n - J_p^n}}\right) u_p^{n,k_p-1} + \frac{\operatorname{mod}(k_T, 2^{J_T^n - J_p^n})}{2^{J_T^n - J_p^n}}\, u_p^{n,k_p} \,.$$

Let Δt_T be the local timestep-length $\Delta\, t^n \,/ 2^{J_T^n}$ of the element $T \in \mathcal{T}_h^n$ and let $\omega_p^n = \{T \in \mathcal{T}_h^n \ : \ p \in T\}$. Taking $w_h = \varphi_p^n \times \chi_p^n$ and performing time integration, the proposed scheme can also be written as follows: *For each* $n = 1, \ldots, N$, *find*

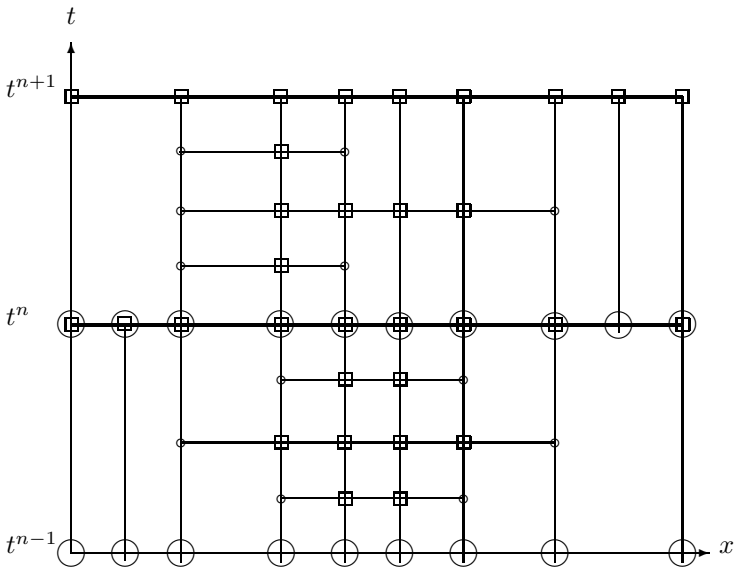

FIG. 2. *Space-time discretization in two successive slabs.*

$u_{h,\Delta t} \in \mathrm{U}^n_{h,\Delta t}$ *such that*

$$\begin{aligned}
&\sum_{T\in\omega_p^n}\sum_{k_T=(k_p-1)2^{J_T^n-J_p^n}+1}^{k_p 2^{J_T^n-J_p^n}} \Delta t_T\left[\left(\frac{u_{h,\Delta t}(t^{n,k_T})-u_{h,\Delta t}(t^{n,k_T-1})}{\Delta t_T},\varphi_p^n\right)_T\right.\\
&\qquad\left.+\left(\kappa\,\nabla\frac{u_{h,\Delta t}(t^{n,k_T})+u_{h,\Delta t}(t^{n,k_T-1})}{2},\nabla\,\varphi_p^n\right)_T\right]\\
&\quad=\sum_{T\in\omega_p^n}\sum_{k_T=(k_p-1)2^{J_T^n-J_p^n}+1}^{k_p 2^{J_T^n-J_p^n}} \Delta t_T\left(\frac{f_{h,\Delta t}(t^{n,k_T})+f_{h,\Delta t}(t^{n,k_T-1})}{2},\varphi_p^n\right)_T \qquad (2.15)
\end{aligned}$$

holds true $\forall\,\varphi_p^n \in \mathrm{V}_h^n$ *and* $\forall k_p = 1,\dots,2^{J_p^n}$.

This is the final formulation that leads to the linear system defining $\nu_{h,\Delta t}$. Furthermore, from (2.14) and (2.15) it follows that $\forall v_h \in \mathrm{V}_h^n$ we have

$$\begin{aligned}
&\sum_{T\in\mathcal{T}_h^n}\sum_{k_T=1}^{2^{J_T^n}} \Delta t_T\left[\left(\frac{u_{h,\Delta t}(t^{n,k_T})-u_{h,\Delta t}(t^{n,k_T-1})}{\Delta t_T},v_h\right)_T\right.\\
&\qquad\left.+\left(\kappa\,\nabla\frac{u_{h,\Delta t}(t^{n,k_T})+u_{h,\Delta t}(t^{n,k_T-1})}{2},\nabla v_h\right)_T\right]\\
&\quad=\sum_{T\in\mathcal{T}_h^n}\sum_{k_T=1}^{2^{J_T^n}} \Delta t_T\left(\frac{f_{h,\Delta t}(t^{n,k_T})+f_{h,\Delta t}(t^{n,k_T-1})}{2},v_h\right)_T. \qquad (2.16)
\end{aligned}$$

In Figure 2 we give a graphical description of the components of the locally substepped method for the 1D case with linear elements, and for the two time intervals I^n and I^{n+1}. The nodes (x_p, t^{n,k_p}) that correspond to the unknowns of the method in each time interval are denoted by boxes. Large circles are used to denote the nodes

(x_p, t^{n-1}) in which the initial conditions for the timesteps I^n are fixed. The hanging nodes in time (x_p, t^{n,k_T}) used in the formulations (2.14)–(2.15) of the method are distinguished by small circles. The thin horizontal lines split the time interval I^n into the $2^{J_T^n}$ subintervals on each element $T \in \mathcal{T}_h^n$. The same symbols are used in the timestep I^{n+1}.

For the sake of simplicity and compactness, from now on, we shall drop the indication of the timeslab n in the notation used for the times within the timesteps $(t^{n,k} \to t^k)$.

2.4. Existence, uniqueness, and stability. In this section a fixed partition in space $\mathcal{T}_h^n$ for all the slabs $\Omega \times I^n$, with $n = 1, \dots, N$, is considered. The time substep-levels J_p^n, $p \in \mathcal{N}_h^n$ do not change for $n = 1, \dots, N$. The main global stability result is stated in the following theorem, whose proof immediately follows from Proposition 2.3.

THEOREM 2.2. *Let $u_{h,\Delta t} \in \mathrm{U}_{h,\Delta t}^n$ be the solution of the locally substepped trapezoidal method* (2.13)*; $\forall n = 1, \dots, N$ the following stability estimate holds true:*

$$\sum_{n=1}^{N} \sum_{T \in \mathcal{T}_h^n} \sum_{k_T=1}^{2^{J_T^n}} \frac{\left\| u_{h,\Delta t}(t^{k_T}) - u_{h,\Delta t}(t^{k_T-1}) \right\|_{0,T}^2}{\Delta t_T} + \sum_{T \in \mathcal{T}_h^N} \left\| \sqrt{\kappa}\, \nabla\, u_{h,\Delta t}(\Xi) \right\|_{0,T}^2$$

$$\leq \sum_{T \in \mathcal{T}_h^1} \left\| \sqrt{\kappa}\, \nabla\, u_{h,\Delta t}(0) \right\|_{0,T}^2 + \sum_{n=1}^{N} \sum_{T \in \mathcal{T}_h^n} \sum_{k_T=1}^{2^{J_T^n}} \frac{\Delta t_T}{4} \left\| f_{h,\Delta t}(t^{k_T}) + f_{h,\Delta t}(t^{k_T-1}) \right\|_{0,T}^2 .$$

PROPOSITION 2.3. *Let $u_{h,\Delta t} \in \mathrm{U}_{h,\Delta t}^n$ be the solution of the locally substepped trapezoidal method* (2.13)*; the following stability estimate holds true:*

$$\sum_{T \in \mathcal{T}_h^n} \sum_{k_T=1}^{2^{J_T^n}} \frac{\left\| u_{h,\Delta t}(t^{k_T}) - u_{h,\Delta t}(t^{k_T-1}) \right\|_{0,T}^2}{\Delta t_T} + \sum_{T \in \mathcal{T}_h^n} \left\| \sqrt{\kappa} \nabla u_{h,\Delta t}(t^n) \right\|_{0,T}^2$$

$$\leq \left\| \sqrt{\kappa} \nabla\, u_{h,\Delta t}(t^{n-1}) \right\|_{0,T}^2 + \sum_{T \in \mathcal{T}_h^n} \sum_{k_T=1}^{2^{J_T^n}} \frac{\Delta t_T}{4} \left\| f_{h,\Delta t}(t^{k_T}) + f_{h,\Delta t}(t^{k_T-1}) \right\|_{0,T}^2 . \tag{2.17}$$

Proof. Let us consider (2.16) and take

$$w_h = \sum_{T \in \mathcal{T}_h^n} \sum_{k_T=1}^{2^{J_T^n}} \frac{u_{h,\Delta t}(x, t^{k_T}) - u_{h,\Delta t}(x, t^{k_T-1})}{\Delta t_T}\, \chi_T(x)\, \chi_{k_T}(t) \in \mathrm{W}_h^n,$$

where χ_T is the characteristic function of the element T in the nth time interval and $\chi_{k_T}(t)$ is the characteristic function of the subintervals $[t^{k_T-1}, t^{k_T}]$ for $k_T = 1, \dots, 2^{J_T^n}$. Applying Cauchy–Schwarz and Young inequalities with a telescopic property we obtain

$$\sum_{T \in \mathcal{T}_h^n} \sum_{k_T=1}^{2^{J_T^n}} \frac{\left\| u_{h,\Delta t}(t^{k_T}) - u_{h,\Delta t}(t^{k_T-1}) \right\|_{0,T}^2}{\Delta t_T} + \frac{1}{2} \sum_{T \in \mathcal{T}_h^n} \left\| \sqrt{\kappa}\, \nabla\, u_{h,\Delta t}(t^n) \right\|_{0,T}^2$$

$$\leq \frac{1}{2} \sum_{T \in \mathcal{T}_h^n} \left\| \sqrt{\kappa}\, \nabla\, u_{h,\Delta t}(t^{n-1}) \right\|_{0,T}^2 + \sum_{T \in \mathcal{T}_h^n} \sum_{k_T=1}^{2^{J_T^n}} \frac{\Delta t_T}{8} \left\| f_{h,\Delta t}(t^{k_T}) + f_{h,\Delta t}(t^{k_T-1}) \right\|_{0,T}^2$$

$$+ \frac{1}{2} \sum_{T \in \mathcal{T}_h^n} \sum_{k_T=1}^{2^{J_T^n}} \frac{\left\| u_{h,\Delta t}(t^{k_T}) - u_{h,\Delta t}(t^{k_T-1}) \right\|_{0,T}^2}{\Delta t_T}.$$

Then, the thesis follows. □

We can easily derive the existence and uniqueness of the numerical solution of the proposed scheme from the stability estimate given in Proposition 2.3. First, we observe that the dimension of the space W_h^n is equal to the dimension of the space $\mathcal{V}_{h,\Delta t}^n$, which contains the unknown component $\nu_{h,\Delta t}$ of the solution $u_{h,\Delta t}$ defined by the equivalent formulations (2.13)–(2.16). Hence, the existence and uniqueness of the solution $\nu_{h,\Delta t}$ and, consequently, of $u_{h,\Delta t}$ for each timeslab easily follow.

2.5. Numerical test. This section concludes with an analysis of the true errors $\| (u_{h,\Delta t}(\Xi) - u_{ex}(\Xi) \|_{0,\Omega}$ for the following 1D problem:

$$\frac{\partial u}{\partial t} - \frac{\partial^2 u}{\partial x^2} = f \qquad \text{in } \Omega \times [0,1], \tag{2.18}$$

$$u(0,t) = u(1,t) = 0 \qquad \forall t \in [0,1], \tag{2.19}$$

$$u(x,0) = u_{ex}(0,x) \qquad \text{in } \Omega = [0,1]. \tag{2.20}$$

The forcing function f is computed so that the exact solution is $u_{ex} = 4x(1-x)\exp(-400(x - 0.5 - 0.1\sin(2\pi(2t + t^2))))$. The spatial mesh is given by 251 uniformly distributed nodes, linear elements are used, and $\Pi_h^n f$ is the piecewise linear interpolation of f in the nodes of the partition. This solution describes a Gaussian peak oscillating around the center of the unit interval. The numerical solutions corresponding to the times $t = 0.125$ and $t = 0.3438$ are reported in Figure 3 with continuous lines.

We consider three different distributions for the substep-levels. In the first test, we use a distribution of J_p^n as described by the dashed line of Figure 3, i.e., we set $J_p^n = 2$ in the central region of the space interval $[x_3 = 0.3, x_4 = 0.7]$, where the peak of the solution moves, $J_p^n = 1$ in a small region $[x_1 = 0.22, x_3) \cup (x_4, x_2 = 0.78]$ around the previous one, and $J_p^n = 0$ outside these regions. We denote this substep level distribution by the tree integers $J_p = 012$ in which the first integer denotes the level of the nodes in $[0, x_1) \cup (x_2, 1]$, the second integer denotes the level of the nodes in $[x_1, x_3) \cup (x_4, x_2]$, and the third integer denotes the level of the nodes in $[x_3, x_4]$. In the second test, we consider a case in which $J_p^n = 1$ in the whole central region, where we had used $J_p^n \neq 0$ in the previous case and $J_p^n = 0$ elsewhere, denoted by $J_p = 011$. Third, we consider a case in which we set $J_p^n = 0$ everywhere, denoted by $J_p = 000$.

The continuous line in Figure 4 reports the true error obtained by setting $J_p = 012$ (first test) and using 4, 8, 16, and 32 time intervals. The dash-dotted line in Figure 4 is the true error corresponding to the case $J_p = 011$ (second test), using 8, 16, 32, and 64 time intervals. The dashed line corresponds to the classical Crank–Nicolson method ($J_p = 000$) with 16, 32, 64, and 128 time intervals. From the curves in Figure 4 it can be seen that the introduction of the substeps into the correct place (the region in which the peak moves) gives the same effect as a global refinement of the timestep, thus proving the viability of the proposed method. The computed order of convergence in time for the different cases is reported in the figure legend, where it can be seen that, in this case, the order of convergence is very close to the second order of the Crank–Nicolson method in all the cases. The two horizontal thin lines plotted in Figure 4 highlight that the errors obtained using $J_p = 000$ and $N = 128$ global time intervals and $J_p = 012$ and $N = 32$ global time intervals are almost equal. The same is true for the errors corresponding to $J_p = 000$ and $N = 64$ global time intervals and $J_p = 012$ and $N = 16$ global time intervals.

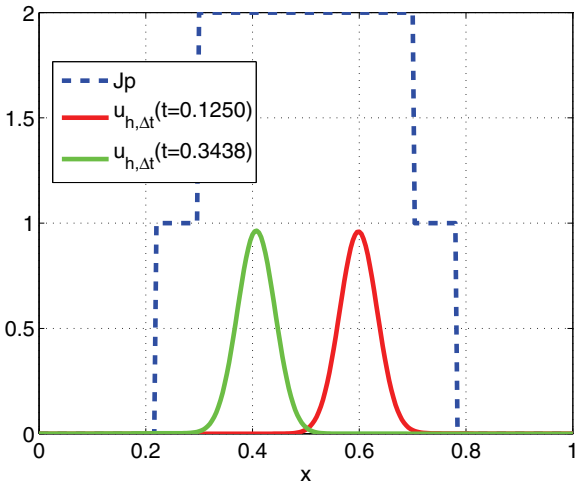

FIG. 3. *Numerical solution at different times obtained from a distribution of the substep-levels with* $J_{p_{max}} = 2$.

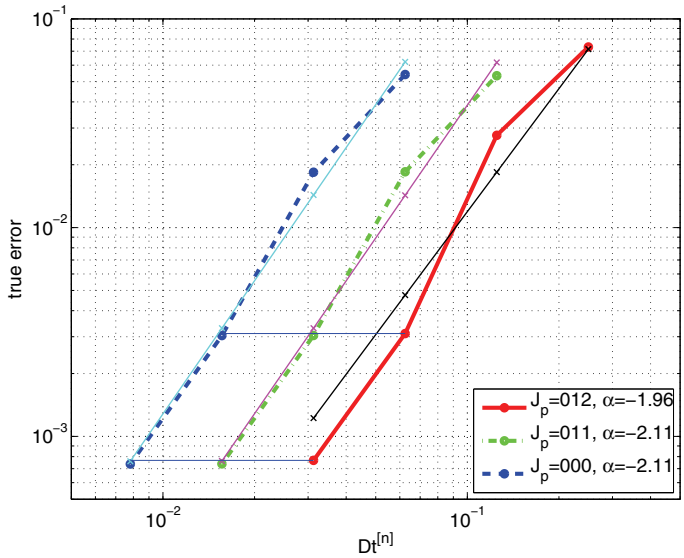

FIG. 4. *True error versus* Δt^n *for different* $J_{p_{max}} = 0, 1, 2$.

3. A residual-based a posteriori error estimator. In this section, within the framework of [6, 15, 18], we derive a residual-based error estimator for our fully discretized model problem (2.16). In particular, we derive global-in-space local-in-time upper and lower bounds.

Remark 3.1. For the a posteriori analysis, we limit ourselves to the case $\Omega \subset \mathbb{R}^d$ with $d = 2$. This a posteriori analysis can be applied to the case $d > 2$ when the diffusivity coefficient κ is constant. Dealing with discontinuous diffusivity coefficients with $d > 2$ requires some restrictions to the mesh produced by the space adaptive strategy. We shall come back to this issue in Remark 3.6.

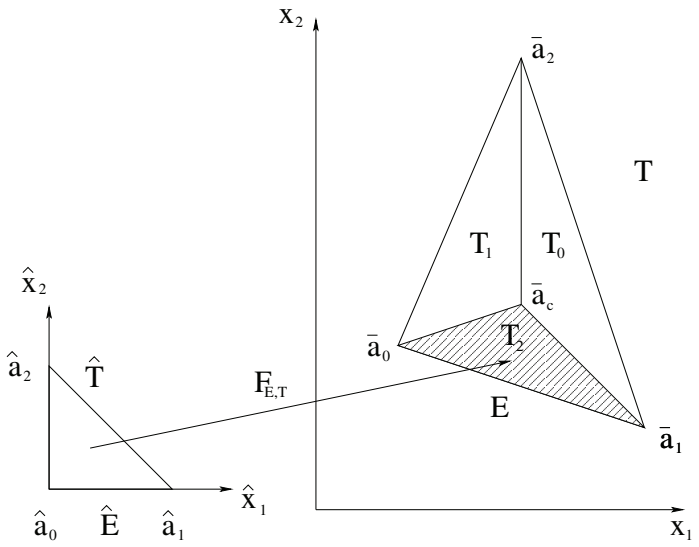

FIG. 5. *The mapping* $F_{E,T} : \hat{T} \to T_2$.

First, we introduce some notations which will be used for the construction of the estimator.

3.1. Definitions and general results. For each timeslab $\Omega \times I^n$, the partition $\mathcal{T}_h^{n-1,n}$ is a common refinement of $\mathcal{T}_h^{n-1}$ and $\mathcal{T}_h^n$, satisfying conformity and minimal-angle conditions and the following *transition condition* or *moderate coarsening condition* [18]: there exists a constant C_{tr} such that

$$\sup_{n=1,\dots,N} \sup_{T \in \mathcal{T}_h^n} \sup_{T_* \in \mathcal{T}_h^{n-1,n} : T_* \subseteq T} \frac{h_T^n}{h_{T_*}^{n-1,n}} \leq C_{tr}, \tag{3.1}$$

where $h_{T_*}^{n-1,n}$ is the diameter of the element $T_* \in \mathcal{T}_h^{n-1,n}$. We denote the set of the edges of any $T \in \mathcal{T}_h^{n-1,n}$ by $\mathcal{E}(T)$; we denote the set of all the edges of the triangulation $\mathcal{T}_h^{n-1,n}$ by $\mathcal{E}_h^{n-1,n} = \cup_{T \in \mathcal{T}_h^{n-1,n}} \mathcal{E}(T)$. Moreover, we split $\mathcal{E}_h^{n-1,n}$ into the form $\mathcal{E}_h^{n-1,n} = \mathcal{E}_{h,\Omega}^{n-1,n} \cup \mathcal{E}_{h,\partial\Omega}^{n-1,n}$ with $\mathcal{E}_{h,\Omega}^{n-1,n} = \{E \in \mathcal{E}_h^{n-1,n} : E \not\subset \partial\Omega\}$, and $\mathcal{E}_{h,\partial\Omega}^{n-1,n} = \{E \in \mathcal{E}_h^{n-1,n} : E \subset \partial\Omega\}$. Similarly, we define the corresponding sets $\mathcal{E}_h^n$, $\mathcal{E}_{h,\Omega}^n$, and $\mathcal{E}_{h,\partial\Omega}^n$ of edges E of $\mathcal{T}_h^n$. For any edge $E \in \mathcal{E}_h^{n-1,n}$ we define $\omega_E^n = \cup_{\{T' \in \mathcal{T}_h^{n-1,n} :\ E \in \mathcal{E}(T')\}} T'$. We associate an orthogonal unit vector n_E with any edge $E \in \mathcal{E}_{h,\Omega}^{n-1,n}$ and denote the jump across E in the direction n_E by $[\![.]\!]_E$. Let us denote the reference element by $\hat{T}$ and the reference edge by $\hat{E}$ as shown on the left in Figure 5. Let λ_i, $i = 0, 1, 2$ be the barycentric coordinates on the reference element, then the *reference element bubble function* is $\hat{b}_{\hat{T}} = 27\lambda_0\lambda_1\lambda_2$, the *reference edge bubble function* is $\hat{b}_{\hat{E}} = 4\hat{x}(1-\hat{x}-\hat{y})$, and $F_T^n : \hat{T} \to T$ is the affine mapping from the reference element to the element $T \in \mathcal{T}_h^{n-1,n}$ [8]. For the sake of simplicity, we drop the superscript n in the mapping symbols. We introduce the *element bubble function* $b_T^n = \hat{b}_{\hat{T}} \circ F_T^{-1}$ for any $T \in \mathcal{T}_h^{n-1,n}$. It should be noted that this bubble function does not depend on time within any timeslab.

Given any $E \in \mathcal{E}_{h,\Omega}^{n-1,n}$, let $T^\sharp$ and $T^\flat$ be the two elements of $\mathcal{T}_h^{n-1,n}$ sharing the edge E ($\omega_E^n = T^\sharp \cup T^\flat$). Let us enumerate the vertices of $T^\sharp$ and $T^\flat$ counterclockwise

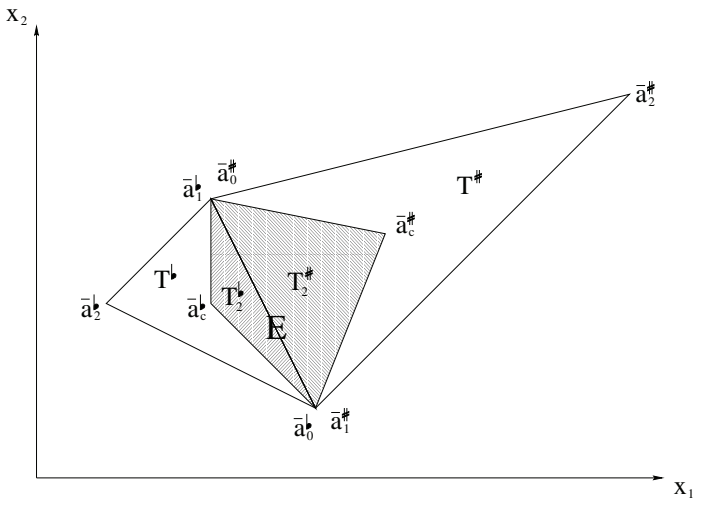

FIG. 6. *The support of the function* b_E^n.

in such a way that the vertices of E are numbered first. Let T be one of the elements $T^\sharp$ or $T^\flat$, assume that E has vertices $\overline{a}_0$ and $\overline{a}_1$, and denote the barycenter of the element T by $\overline{a}_c = (x_c, y_c)$; let us partition T into the elements T_0, T_1, T_2 with T_2 having E as a side (see Figure 5 (right)). Let $F_{E,T} : \hat{T} \to T_2$ be the invertible affine mapping that maps the reference element $\hat{T}$ onto the element T_2: $F_{E,T}(\hat{x}, \hat{y}) = \overline{a}_0 \ \lambda_0(\hat{x}, \hat{y}) + \overline{a}_1 \ \lambda_1(\hat{x}, \hat{y}) + \overline{a}_c \ \lambda_2(\hat{x}, \hat{y}) \ \forall (\hat{x}, \hat{y}) \in \hat{T}$. We then define the *edge bubble function* b_E^n by patching the two bubble functions: $b_{E,T^\sharp}^n = \hat{b}_{\hat{E}} \circ F_{E,T^\sharp}^{-1}$, $b_{E,T^\flat}^n = \hat{b}_{\hat{E}} \circ F_{E,T^\flat}^{-1}$, each one being nonzero only on $T_2^\sharp$ and $T_2^\flat$, respectively. Finally, for an internal edge E let us define the set $\mathring{\omega}_E^n = T_2^\sharp \cup T_2^\flat$ (dashed area in Figure 6). For the boundary edge E that belongs only to the element T, we naturally identify b_E^n with $b_{E,T}^n = \hat{b}_{\hat{E}} \circ F_{E,T}^{-1}$.

With this definition of edge bubble functions, we have a set of orthogonal functions. This property is also true for the set of element bubble functions.

Furthermore, for the reference edge $\hat{E}$, we define the extension operator $\hat{\mathcal{P}}_{\hat{E}} : \mathbb{P}_i(\hat{E}) \to \mathbb{P}_i(\hat{T})$, which extends a polynomial of degree i, defined on the edge $\hat{E}$, to a polynomial of the same degree, defined on $\hat{T}$, with constant values along lines orthogonal to the edge $\hat{E}$. We then define the extension operator $\mathcal{P}_E : \mathbb{P}_i(E) \to \mathbb{P}_i(\mathring{\omega}_E^n)$, which extends a polynomial of degree i, defined on the edge E, to a piecewise polynomial of the same degree, defined on $\mathring{\omega}_E^n$, by patching the two operators: $\mathcal{P}_{E|_{T^\sharp}} = F_{E,T_2^\sharp} \circ \hat{\mathcal{P}}_{\hat{E}} \circ F_{E,T_2^\sharp|_E}^{-1}$, $\mathcal{P}_{E|_{T^\flat}} = F_{E,T_2^\flat} \circ \hat{\mathcal{P}}_{\hat{E}} \circ F_{E,T_2^\flat|_E}^{-1}$. The extension operator $\mathcal{P}_E$ is continuous, but not $\mathcal{C}^1$ in $\mathring{\omega}_E^n$. In the following we will need to collect all the elements belonging to some set $\mathring{\omega}_E^n$; therefore, let us define $\mathcal{T}_{h,\mathring{\omega}}^{n-1,n} = \{T_2 \in \mathring{\omega}_E^n : E \in \mathcal{E}_h^{n-1,n}\}$.

The symbol $a \precsim b$ means that there exists a constant c that is independent of any meshsize, timestep, parameter, or jump of parameters so that $a \leq c\, b$.

In the following, κ_T denotes the constant value of κ in the element $T \in \mathcal{T}_h^n$, and $\hat{\kappa}_{\omega_E^n}$ is the maximum of the values of κ_T over the two elements $T \in \mathcal{T}_h^n$ that share the edge E (we will use the same symbol to denote the maximum of κ_T over the two elements $T \in \mathcal{T}_h^{n-1,n}$ that share the edge $E \in \mathcal{E}_h^{n-1,n}$, and it will be clear from the context which situation we are referring to). Moreover, we shall use a modified *quasi-*

interpolation operator $I_h : \mathrm{V} \to \mathrm{V}_h^n$ like Clément's quasi-interpolation operator [9]. The definition of this kind of interpolation operator requires the quasi-monotonicity hypothesis [11, 14] of $\kappa(x)$ with respect to any vertex x_h^n of the triangulation $\mathcal{T}_h^n$. This hypothesis implies the existence of "robust" interpolation estimates [5, 11, 14]. For any subset $\omega \subseteq \overline{\Omega}$, let $\mathcal{N}_h^n(\omega)$ be the set of vertices x of the triangulation $\mathcal{T}_h^n$ so that $x \in \omega$; let $\omega_{x_h^n}$ be the set of the elements that have x_h^n as a vertex. Moreover, let $\hat{T}_{x_h^n}$ be an element of $\omega_{x_h^n}$ where the coefficient κ_T achieves its maximum in $\omega_{x_h^n}$. We recall the following definition of quasi-monotonicity for $\kappa(x)$ from [14], where further details can be referenced.

DEFINITION 3.2 (quasi-monotonicity). *The distribution of coefficients κ_T, $T \in \omega_{x_h^n}$ is said to be quasi-monotone with respect to the vertex $x_h^n \in \mathcal{N}_h^n(\overline{\Omega})$ if, for each element $T \in \omega_{x_h^n}$, there exists a Lipschitz set $\tilde{\omega}_{T,x_h^n}$ that contains elements $T' \in \omega_{x_h^n}$ so that*

- *if $x_h^n \in \Omega$, then $T \cup \hat{T}_{x_h^n} \subseteq \tilde{\omega}_{T,x_h^n}$ and $\kappa_T \leq \kappa_{T'}\ \forall T' \in \tilde{\omega}_{T,x_h^n}$;*
- *if $x_h^n \in \partial\Omega$, then $T \subseteq \tilde{\omega}_{T,x_h^n}$, $\left|\partial\,\tilde{\omega}_{T,x_h^n} \cap \partial\Omega\right| > 0$, and $\kappa_T \leq \kappa_{T'}\ \forall T' \in \tilde{\omega}_{T,x_h^n}$.*

Let the distribution of coefficients κ_T, $T \in \mathcal{T}_h^n$ be quasi-monotone with respect to each point $x_h^n \in \mathcal{N}_h^n(\overline{\Omega})$. For an element $T \in \mathcal{T}_h^n$ and an edge $E \in \mathcal{E}_{h,\Omega}^n$, let us define two sets containing some neighboring elements $\tilde{\omega}_T^n = \cup_{x_h^n \in \mathcal{N}_h^n(T)} \tilde{\omega}_{T,x_h^n}$, $\tilde{\omega}_E^n = \cup_{x_h^n \in \mathcal{N}_h^n(T_E)} \tilde{\omega}_{T,x_h^n}$, where T_E is the element of the two elements sharing E, where κ_T achieves the maximum.

DEFINITION 3.3 (quasi-interpolation operator; [5, 11, 14]). *Let the distribution of coefficients κ_T, $T \in \mathcal{T}_h^n$ be quasi-monotone. We then define the quasi-interpolation operator $I_h^n : V \to \mathrm{V}_h^n$ as*

$$I_h^n v = \sum_{i=1}^{\dim \mathcal{N}_h^n(\Omega)} \lambda_i(x) p_{x_{h,i}^n}, \qquad p_{x_{h,i}^n} = \frac{1}{\hat{T}_{x_{h,i}^n}} \int_{\hat{T}_{x_{h,i}^n}} v \mathrm{d}\Omega \quad \forall\, x_{h,i}^n \in \mathcal{N}_h^n(\Omega).$$

Let $p_x = 0$ for the nodal points $x \in \partial\Omega$.

We recall the following results from [14].

LEMMA 3.4. *Let $T \in \mathcal{T}_h^n$ and $E \in \mathcal{E}_h^n$ be arbitrary. Let the quasi-monotonicity condition be satisfied with respect to any vertex x_h^n of T or T_E. We thus obtain the following interpolation error estimates:*

$$\| v - I_h^n v \|_{0,T} \leq \tilde{C}l_R \frac{h_T^n}{\sqrt{\kappa_T}} \sum_{T' \in \tilde{\omega}_T^n} \| \sqrt{\kappa_{T'}} \nabla v \|_{0,T'} \qquad \forall v \in \mathrm{H}^1(\tilde{\omega}_T^n), \tag{3.2}$$

$$| v - I_h^n v |_{1,T} \leq \tilde{C}l_{R,1} \frac{1}{\sqrt{\kappa_T}} \sum_{T' \in \tilde{\omega}_T^n} \| \sqrt{\kappa_{T'}} \nabla v \|_{0,T'} \qquad \forall v \in \mathrm{H}^1(\tilde{\omega}_T^n), \tag{3.3}$$

$$\| v - I_h^n v \|_{0,E} \leq \tilde{C}l_E \frac{\sqrt{h_E^n}}{\sqrt{\hat{\kappa}_{\omega_E^n}}} \sum_{T' \in \tilde{\omega}_E^n} \| \sqrt{\kappa_{T'}} \nabla v \|_{0,T'} \qquad \forall v \in \mathrm{H}^1(\tilde{\omega}_E^n), \tag{3.4}$$

where the constants $\tilde{C}l_R$, $\tilde{C}l_{R,1}$, and $\tilde{C}l_E$ depend only on the smallest angle in the triangulation.

For each element $T_* \in \mathcal{T}_h^{n-1,n}$ so that $T_* \subseteq T \in \mathcal{T}_h^n$, we define the set of elements $\tilde{\omega}_{T_*}^n = \{T' \in \mathcal{T}_h^{n-1,n} : T' \subseteq T'' \in \tilde{\omega}_T^n \subseteq \mathcal{T}_h^n\}$, i.e., the set of elements of $\mathcal{T}_h^{n-1,n}$ contained in, or equal to, an element $T'' \in \mathcal{T}_h^n$ belonging to $\tilde{\omega}_T^n$. Moreover, if $E_* = E \in \mathcal{E}_h^n$ or if $E_* \subset E \in \mathcal{E}_h^n$, we then define $\tilde{\omega}_{E_*}^n = \{T' \in \mathcal{T}_h^{n-1,n} : T' \subseteq T'' \in \tilde{\omega}_E^n \subseteq \mathcal{T}_h^n\}$, or else if $E_* \in \mathcal{E}_h^{n-1,n} \setminus \mathcal{E}_h^n$ and $E_* \not\subset E \in \mathcal{E}_h^n$, let $T \in \mathcal{T}_h^n$ be the element so that E_* is

inside T, then $\tilde{\omega}^n_{E_*} = \{T' \in \mathcal{T}_h^{n-1,n} : T' \subseteq T'' \in \tilde{\omega}^n_T \subseteq \mathcal{T}_h^n\}$, i.e., the sets of elements of $\mathcal{T}_h^{n-1,n}$ contained in, or equal to, an element of $\tilde{\omega}^n_E$ or $\tilde{\omega}^n_T$, respectively.

We recall the following results from [6], which extend the results of Lemma 3.4 to the elements and edges of the common refinement $\mathcal{T}_h^{n-1,n}$.

LEMMA 3.5. *Let $T_* \in \mathcal{T}_h^{n-1,n}$ and $E_* \in \mathcal{E}_h^{n-1,n}$ be arbitrary. We thus obtain the following interpolation error estimates:*

$$\| v - I_h^n v \|_{0,T_*} \leq Cl_R \frac{h_{T_*}^{n-1,n}}{\sqrt{\kappa_{T_*}}} \left\| \sqrt{\kappa}\, \nabla v \right\|_{0,\tilde{\omega}^n_{T_*}} \qquad \forall v \in \mathrm{H}^1(\tilde{\omega}^n_{T_*}), \tag{3.5}$$

$$\| v - I_h^n v \|_{0,E_*} \leq Cl_E \frac{\sqrt{h_{E_*}^{n-1,n}}}{\sqrt{\hat{\kappa}_{\omega^n_{E_*}}}} \left\| \sqrt{\kappa}\, \nabla v \right\|_{0,\tilde{\omega}^n_{E_*}} \qquad \forall v \in \mathrm{H}^1(\tilde{\omega}^n_{E_*}), \tag{3.6}$$

where the constants Cl_R and Cl_E depend only on the smallest angle in the triangulation $\mathcal{T}_h^n$ and the constant C_{tr}.

Remark 3.6. Here we come back to the issue introduced in Remark 3.1 to explain the difficulty of having $d > 2$ with discontinuous coefficients. In Lemma 3.5 we have to ensure that the triangulation $\mathcal{T}_h^{n-1,n}$ always satisfies the quasi-monotonicity condition with respect to any vertex of the triangulation $\mathcal{T}_h^{n-1,n}$. This is always true for $\Omega \subset \mathbb{R}^2$ as the triangulation $\mathcal{T}_h^{n-1,n}$ is a refinement of two triangulations $\mathcal{T}_h^{n-1}$ and $\mathcal{T}_h^n$, both of them satisfying the quasi-monotonicity condition, which is preserved by refinement. When $d > 2$, the refinement does not preserve the quasi-monotonicity condition and a suitable refinement algorithm or additional hypotheses for the construction of $\mathcal{T}_h^n$, which we do not investigate here, have to be applied to guarantee the quasi-monotonicity condition for $\mathcal{T}_h^{n-1,n}$ required in the present analysis. We remark that, if we consider constant diffusivity coefficients, quasi-monotonicity assumptions are always satisfied. In this case, the entire present a posteriori analysis can be obtained for $d > 2$ resorting to the classical quasi-interpolation operators properties instead of to Lemmas 3.4 and 3.5.

Let us consider the spaces $\mathrm{H}^1_0(\Omega)$ and $\mathrm{H}^{-1}(\Omega)$, respectively, equipped with the norms

$$\| v \|^2_{\kappa,1} = \left\| \sqrt{\kappa}\, \nabla v \right\|^2_0 = \int_\Omega \kappa(x)\, \nabla v \cdot \nabla v \mathrm{d}\Omega, \qquad \| F \|_{\kappa,-1} = \sup_{v \in \mathrm{H}^1_0(\Omega)} \frac{\langle F\,,\, v \rangle}{\| v \|_{\kappa,1}}.$$

In the following we define $J^n_{T_*} = J^n_T$ for each element $T_* \in \mathcal{T}_h^{n-1,n}$, so that $T_* \subseteq T \in \mathcal{T}_h^n$, and, for each edge $E_* \in \mathcal{E}_{h,\Omega}^{n-1,n}$, we define the subinterval level $J^n_{E_*}$ as the maximum between the $J^n_{T_*}$ of the elements sharing the edge E_*. For the sake of simplicity, we shall use the shorter notation J_{T_*} and J_{E_*} instead of $J^n_{T_*}$ and $J^n_{E_*}$. Moreover, we define $\Delta t_{T_*} = \Delta t\,/2^{J_{T_*}}\ \forall\, T_* \in \mathcal{T}_h^{n-1,n}$ and $\Delta t_{E_*} = \Delta t\,/2^{J_{E_*}}\ \forall\, E_* \in \mathcal{E}_{h,\Omega}^{n-1,n}$.

DEFINITION 3.7. *Let us define the residual in the elements $T_* \in \mathcal{T}_h^{n-1,n}$ of our approximation $u_{h,\Delta t}$ in each interval $[t^{k_{T_*}-1}, t^{k_{T_*}}]\ \forall k_{T_*} = 1, \ldots, 2^{J_{T_*}}$:*

$$R^{k_{T_*}}_{T_*} = \frac{\partial\, u_{h,\Delta t}(t)}{\partial t} - \kappa_{T_*} \triangle \frac{u_{h,\Delta t}(t^{k_{T_*}}) + u_{h,\Delta t}(t^{k_{T_*}-1})}{2} - \left. \frac{f_{h,\Delta t}(t^{k_{T_*}}) + f_{h,\Delta t}(t^{k_{T_*}-1})}{2} \right|_{T_*},$$

where

$$\frac{\partial\, u_{h,\Delta t}(t)}{\partial t} = \frac{u_{h,\Delta t}(x, t^{k_{T_*}}) - u_{h,\Delta t}(x, t^{k_{T_*}-1})}{\Delta t_{T_*}} \qquad \forall t \in \left(t^{k_{T_*}-1}, t^{k_{T_*}}\right).$$

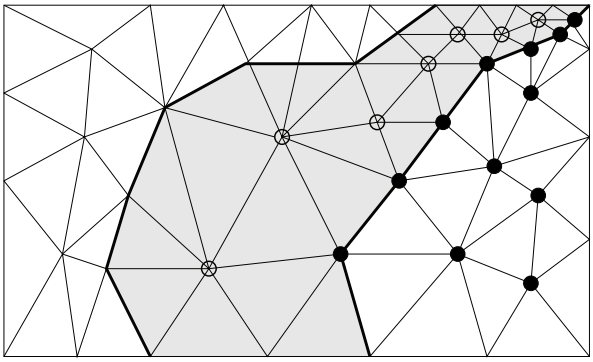

FIG. 7. *Representation of $\mathcal{N}^n_{h,tr}$ and $\mathcal{T}^n_{h,tr}$: dark bullets represent nodes with equal high substep-level, all the other nodes have equal lower substep-level. Circles represent the nodes of the set $\mathcal{N}^n_{h,tr}$, dashed triangles represent the set $\mathcal{T}^n_{h,tr}$.*

Let us also define the interelement jumps on the edges $E_* \in \mathcal{E}^{n-1,n}_{h,\Omega}$ of our approximation $u_{h,\Delta t}$ on the two elements $T' \in \mathcal{T}^{n-1,n}_h$ that share E_* in each interval $[t^{k_{E_*}-1}, t^{k_{E_*}}]$ $\forall k_{E_*} = 1, \dots, 2^{J_{E_*}}$:

$$J^{k_{E_*}}_{E_*} = \left[\!\!\left[\frac{\kappa_{T'}}{2} \frac{\partial (u_{h,\Delta t}(t^{k_{E_*}}) + u_{h,\Delta t}(t^{k_{E_*}-1}))}{\partial n_{E_*}} \right]\!\!\right]_{E_*}.$$

NOTATION 3.8. *For the sake of compactness, we will use the symbols $\sum_{T_*,k_{T_*}}$ instead of the double sum $\sum_{T_* \in \mathcal{T}^{n-1,n}_h} \sum_{k_{T_*}=1}^{2^{J_{T_*}}}$ and $\sum_{E_*,k_{E_*}}$ instead of $\sum_{E_* \in \mathcal{E}^{n-1,n}_{h,\Omega}} \sum_{k_{E_*}=1}^{2^{J_{E_*}}}$. Moreover, we will set*

$$\mathcal{M}^{k_{T_*}}(u_{h,\Delta t}) = \frac{u_{h,\Delta t}(t^{k_{T_*}}) + u_{h,\Delta t}(t^{k_{T_*}-1})}{2},\ \mathcal{M}^{k_{T_*}}(f_{h,\Delta t}) = \frac{f_{h,\Delta t}(t^{k_{T_*}}) + f_{h,\Delta t}(t^{k_{T_*}-1})}{2}.$$

DEFINITION 3.9. *Given the solution $u_{h,\Delta t}$ in the time interval I^n, let us define the following functional $r^n_\Omega : \mathrm{L}^2(I^n, \mathrm{V}^n_h) \to \mathrm{L}^1(I^n)$:*

$$r^n_\Omega(v_h) = \sum_{T_*,k_{T_*}} \left(\frac{\partial u_{h,\Delta t}(t)}{\partial t}, v_h(t) \right)_{T_*} + \sum_{T_*,k_{T_*}} \left(\kappa \nabla \mathcal{M}^{k_{T_*}}(u_{h,\Delta t})\, \chi_{k_{T_*}}(t), \nabla v_h(t) \right)_{T_*}$$
$$- \sum_{T_*,k_{T_*}} \left(\mathcal{M}^{k_{T_*}}(f_{h,\Delta t})\, \chi_{k_{T_*}}(t), v_h(t) \right)_{T_*}. \tag{3.7}$$

DEFINITION 3.10. *Let us define the sets*

$$\mathcal{N}^n_{h,tr} = \left\{ p \in \mathcal{N}^n_h \ :\ \exists p' \in \mathcal{N}^n_h \text{ s.t. } p' \in \overline{\operatorname{supp} \varphi^n_p} \text{ with } J^n_p < J^n_{p'} \right\},$$
$$\mathcal{T}^n_{h,tr} = \left\{ T \in \mathcal{T}^n_h \ :\ \exists p \in T \cap \mathcal{N}^n_{h,tr} \right\}, \quad \mathcal{T}^{n-1,n}_{h,tr} = \left\{ T \in \mathcal{T}^{n-1,n}_h \ :\ T \cap \mathcal{T}^n_{h,tr} \neq \emptyset \right\},$$
$$\mathrm{V}^n_{h,tr} = span \left\{ \varphi^n_p \in \mathrm{V}^n_h \ :\ \exists p \in \mathcal{N}^n_{h,tr} \right\}, \quad \mathrm{V}^n_{h,cn} = span \left\{ \varphi^n_p \in \mathrm{V}^n_h \ :\ \varphi^n_p \notin \mathrm{V}^n_{h,tr} \right\}.$$

The set $\mathcal{N}^n_{h,tr}$ is the set of the nodes of the partition $\mathcal{T}^n_h$ whose basis functions have a support with a nonempty intersection with the support of nodes with a higher substep-level. The set $\mathcal{T}^n_{h,tr}$ contains the elements for which at least one of the nodes

has a basis function φ_p^n interacting with a basis function $\varphi_{p'}^n$ with a higher level $J_{p'}^n$. Figure 7 exhibits a description of these sets on a simple mesh with only two substep-levels. Being that $\mathrm{V}_h^n = \mathrm{V}_{h,tr}^n \oplus \mathrm{V}_{h,cn}^n$, we can write $v_h = v_{h,tr} + v_{h,cn}$, where $v_{h,tr} \in \mathrm{L}^2(I^n, \mathrm{V}_{h,tr}^n)$ has homogeneous boundary conditions on the boundaries of $\mathcal{T}_{h,tr}^n$ $\forall t \in I^n$ and $v_{h,cn} \in \mathrm{L}^2(I^n, \mathrm{V}_{h,cn}^n)$. Resorting to the formulation (2.15), we can see that $r_\Omega^n(v_{h,cn}) = 0$ implies $r_\Omega^n(v_h) = r_\Omega^n(v_{h,tr})$.

We define the quantities that are local either in each subtimestep or in each timestep as local-in-time.

DEFINITION 3.11. *Let us define the following local-in-space local-in-time estimators:*

$$\left(\eta_{R,T_*}^{k_{T_*}}\right)^2 = \Delta t_{T_*} \left(h_{T_*}^{n-1,n}\right)^2 \left\| \frac{1}{\sqrt{\kappa_{T_*}}} R_{T_*}^{k_{T_*}} \right\|_{0,T_*}^2 + \frac{1}{2} \sum_{E_* \in \mathcal{E}(T_*) \cap \mathcal{E}_{h,\Omega}^{n-1,n}} \sum_{k_{E_*} = (k_{T_*}-1)2^{(J_{E_*} - J_{T_*})}+1}^{k_{T_*} 2^{(J_{E_*} - J_{T_*})}} \Delta t_{E_*} \, h_{E_*}^{n-1,n} \left\| \frac{1}{\sqrt{\hat{\kappa}_{\omega_{E_*}^n}}} J_{E_*}^{k_{E_*}} \right\|_{0,E_*}^2,$$

$$\begin{aligned}\left(\eta_{\nabla,T_*}^{k_{T_*}}\right)^2 &= \int_{t^{k_{T_*}-1}}^{t^{k_{T_*}}} \left\| \sqrt{\kappa_{T_*}} \, \nabla \left(u_{h,\Delta t} - \mathcal{M}^{k_{T_*}}(u_{h,\Delta t})\right) \right\|_{0,T_*}^2 \mathrm{d}t \\ &= \int_{t^{k_{T_*}-1}}^{t^{k_{T_*}}} \left\| \sqrt{\kappa_{T_*}} \left[\frac{t - t^{k_{T_*}-1}}{t^{k_{T_*}} - t^{k_{T_*}-1}} - \frac{1}{2} \right] \nabla \big(u_{h,\Delta t}(t^{k_{T_*}}) - u_{h,\Delta t}(t^{k_{T_*}-1})\big) \right\|_{0,T_*}^2 \mathrm{d}t \\ &= \frac{\Delta t_{T_*}}{12} \left\| u_{h,\Delta t}(t^{k_{T_*}}) - u_{h,\Delta t}(t^{k_{T_*}-1}) \right\|_{\kappa,1,T_*}^2,\end{aligned}$$

$$\left(\eta_{R,T_*}^n\right)^2 = \sum_{k_{T_*}=1}^{2^{J_{T_*}}} \left(\eta_{R,T_*}^{k_{T_*}}\right)^2, \qquad \left(\eta_{\nabla,T_*}^n\right)^2 = \sum_{k_{T_*}=1}^{2^{J_{T_*}}} \left(\eta_{\nabla,T_*}^{k_{T_*}}\right)^2.$$

Then, we define the following global-in-space and local-in-time estimators

$$(\eta_R^n)^2 = \sum_{T_* \in \mathcal{T}_h^{n-1,n}} \left(\eta_{R,T_*}^n\right)^2, \qquad (\eta_\nabla^n)^2 = \sum_{T_* \in \mathcal{T}_h^{n-1,n}} \left(\eta_{\nabla,T_*}^n\right)^2,$$

$$(\eta_\delta^n)^2 = \int_{t^{n-1}}^{t^n} \|r_\Omega^n\|_{\kappa,-1,\mathcal{T}_h}^2 \mathrm{d}t = \left[\sup_{v_h \in \mathrm{L}^2(I^n, \mathrm{V}_h^n)} \frac{\int_{t^{n-1}}^{t^n} r_\Omega^n(v_h(t)) \mathrm{d}t}{\sqrt{\int_{t^{n-1}}^{t^n} \| v_h(t) \|_{\kappa,1}^2 \mathrm{d}t}} \right]^2,$$

$$\left(\eta_{f,\Delta t}^n\right)^2 = \int_{t^{n-1}}^{t^n} \left\| \Pi_h^n f - \sum_{T_*, k_{T_*}} \mathcal{M}^{k_{T_*}}(f_{h,\Delta t}) \chi_{T_*} \chi_{k_{T_*}}(t) \right\|_{\kappa,-1}^2 \mathrm{d}t,$$

$$\left(\eta_{f,\Pi_h}^n\right)^2 = \int_{t^{n-1}}^{t^n} \| f - \Pi_h^n f \|_{\kappa,-1}^2 \mathrm{d}t, \qquad \left(\eta_f^n\right)^2 = \left(\eta_{f,\Delta t}^n\right)^2 + \left(\eta_{f,\Pi_h}^n\right)^2.$$

Let us define the error of our approximation $u_{h,\Delta t}$ in the interval I^n as $e = u_{h,\Delta t} - u$. In what follows, we derive upper and lower bounds for the error involving the following norm:

$$\| e \|_{\kappa,I^n} = \left(\int_{t^{n-1}}^{t^n} \left\| \frac{\partial e}{\partial t} \right\|_{\kappa,-1}^2 \mathrm{d}t + \int_{t^{n-1}}^{t^n} \| e \|_{\kappa,1}^2 \mathrm{d}t \right)^{\frac{1}{2}}.$$

Remark 3.12. According to the considerations of [6, 15, 18], we can say that η_R^n is a space error estimator related to the triangulation $\mathcal{T}_h^n$, whereas η_∇^n gives information on the error due to time discretization. In particular, as the terms $\eta_{\nabla,T_*}^{k_{T_*}}$ are local in the element T_* and in the subtimesteps k_{T_*}, they give a measure of the accuracy of the time discretization in the subintervals $(t^{k_{T_*}-1}, t^{k_{T_*}})$ on T_*.

The comprehension of the meaning of η_δ^n is more delicate. This term is a measure of the effect of the transitions in the time substepping partition of the nodes. In particular, it is large if, on some elements in which the nodes have different levels, the forcing function displays significant variations or the solution displays significant changes in the values or in the slope.

The quantity η_f^n is an estimator of the data approximation error and can be split into two terms: $\eta_{f,\Pi_h^n}^n$, which essentially gives information on the space data approximation error, and $\eta_{f,\Delta t^n}^n$, which is a time data approximation error.

Remark 3.13. The quantity η_δ^n is defined via a supremum over a finite dimensional set of functions in space and over L^2 functions in time. We remark that in the definition (3.7) we perform a space scalar product between the test function $v_h \in \mathrm{L}^2(I^n, \mathrm{V}_h^n)$ and given functions which are piecewise constant in time on each time-interval $[t^{k_T-1}, t^{k_T}]$. The supremum in the definition of η_δ^n defines an L^2-norm in time, but the test function v_h that realizes the supremum has to be piecewise constant in time on each $[t^{k_T-1}, t^{k_T}]$. This can easily be proved observing that

$$\int_{t^{n-1}}^{t^n} r_\Omega^n(v_h)\mathrm{d}t = \sum_{T_*,k_{T_*}} \int_{T_*} \left[\left(\frac{\partial\, u_{h,\Delta t}(t)}{\partial t} - \mathcal{M}^{k_{T_*}}(f_{h,\Delta t}) \right) \int_{t^{k_{T_*}-1}}^{t^{k_{T_*}}} v_h \mathrm{d}t \right.$$
$$\left. + \kappa\, \nabla\, \mathcal{M}^{k_{T_*}}(u_{h,\Delta t})\, \nabla \int_{t^{k_{T_*}-1}}^{t^{k_{T_*}}} v_h \mathrm{d}t \right]$$

and the stability property of the L^2 projection. With this additional information the definition of η_δ^n involves a supremum over a finite dimensional space and is, in principle, computable.

3.2. Upper bound. In this section we prove that the terms η_R^n, η_∇^n, η_δ^n, and η_f^n bound the error of the discrete solution with respect to the exact solution of the continuous variational formulation.

THEOREM 3.14. *Under the assumptions on the continuous problem* (2.4) *and on the discrete formulation* (2.13)*, for each* $n = 1, \ldots, N$ *there exists a constant* $\tilde{C}_{n-1}^n$ *independent of any meshsize, timestep, and problem-parameter, and depending only on the smallest angle of the triangulation* $\mathcal{T}_h^n$ *and on the constant* C_{tr} *such that*

$$\| e(t^n) \|_0^2 + \int_{t^{n-1}}^{t^n} \left\| \sqrt{\kappa}\, \nabla\, e(t) \right\|_0^2 \mathrm{d}t \le \left\| e(t^{n-1}) \right\|_0^2$$
$$+ \tilde{C}_{n-1}^n \left[(\eta_R^n)^2 + (\eta_\nabla^n)^2 + (\eta_\delta^n)^2 + \left(\eta_f^n\right)^2 \right]. \tag{3.8}$$

Proof. Let us define

$$E^n_{h,\Delta t} = \int_{t^{n-1}}^{t^n} \left[\left\langle \frac{\partial\, e(t)}{\partial t}, e(t) \right\rangle + (\kappa\, \nabla\, e(t), \nabla\, e(t)) \right] \mathrm{d}t \tag{3.9}$$

$$= \frac{1}{2} \| e(t^n) \|_0^2 - \frac{1}{2} \| e(t^{n-1}) \|_0^2 + \int_{t^{n-1}}^{t^n} \| \sqrt{\kappa}\, \nabla\, e(t) \|_0^2 \mathrm{d}t \tag{3.10}$$

$$= \int_{t^{n-1}}^{t^n} \left[\left(\frac{\partial\, u_{h,\Delta t}(t)}{\partial t}, e(t) \right) + (\kappa\, \nabla\, u_{h,\Delta t}(t), \nabla\, e(t)) - (f(t), e(t)) \right] \mathrm{d}t\,. \tag{3.11}$$

We add and subtract to (3.11) the quantity $\int_{t^{n-1}}^{t^n} r^n_\Omega\, (I^n_h e(t)) \mathrm{d}t$ and we get

$$\begin{aligned}
E^n_{h,\Delta t} = & \sum_{T_*, k_{T_*}} \int_{t^{k_{T_*}-1}}^{t^{k_{T_*}}} \left(\frac{\partial\, u_{h,\Delta t}(t)}{\partial t} - \mathcal{M}^{k_{T_*}}(f_{h,\Delta t}), e(t) - I^n_h e(t) \right)_{T_*} \mathrm{d}t \\
& + \sum_{T_*, k_{T_*}} \int_{t^{k_{T_*}-1}}^{t^{k_{T_*}}} \left(\nabla\, \mathcal{M}^{k_{T_*}}(u_{h,\Delta t}), \nabla (e(t) - I^n_h e(t)) \right)_{T_*} \mathrm{d}t \\
& + \sum_{T_*, k_{T_*}} \int_{t^{k_{T_*}-1}}^{t^{k_{T_*}}} \left(\frac{\partial\, u_{h,\Delta t}(t)}{\partial t} - \mathcal{M}^{k_{T_*}}(f_{h,\Delta t}), I^n_h e(t) \right)_{T_*} \mathrm{d}t \\
& + \sum_{T_*, k_{T_*}} \int_{t^{k_{T_*}-1}}^{t^{k_{T_*}}} \left(\kappa\, \nabla\, \mathcal{M}^{k_{T_*}}(u_{h,\Delta t}), \nabla\, I^n_h e(t) \right)_{T_*} \mathrm{d}t \\
& + \sum_{T_*, k_{T_*}} \int_{t^{k_{T_*}-1}}^{t^{k_{T_*}}} \left(\kappa \nabla \left[u_{h,\Delta t}(t) - \mathcal{M}^{k_{T_*}}(u_{h,\Delta t}) \right], \nabla\, e(t) \right)_{T_*} \mathrm{d}t \\
& - \int_{t^{n-1}}^{t^n} (f(t) - \Pi^n_h\, f(t), e(t)) \mathrm{d}t \\
& - \int_{t^{n-1}}^{t^n} \left(\left[\Pi^n_h\, f(t) - \sum_{T_*, k_{T_*}} \mathcal{M}^{k_{T_*}}(f_{h,\Delta t})\, \chi_{T_*} \chi_{k_{T_*}}(t) \right], e(t) \right) \mathrm{d}t\,.
\end{aligned}$$

We apply integration by parts, Cauchy–Schwarz inequality, Lemma 3.5, and Young's inequality with a suitable choice of constants, getting the thesis. ∎

The result given by Theorem 3.14 is an upper bound of the error measured in the $\mathrm{L}^2(\Omega)$-norm at time t^n and in the $\mathrm{L}^2(I^n; \mathrm{H}^1_0(\Omega))$-norm. We can also get an upper bound in the $\mathrm{L}^2(I^n; \mathrm{H}^{-1}(\Omega))$-norm for $\partial\, e\, / \partial t$.

THEOREM 3.15. *Under the assumptions on the continuous problem* (2.4) *and on the discrete formulation* (2.13)*, for each* $n = 1, \ldots, N$ *we have*

$$\int_{t^{n-1}}^{t^n} \left\| \frac{\partial\, e}{\partial t} \right\|^2_{\kappa,-1} \mathrm{d}t \le C \left[(\eta^n_R)^2 + (\eta^n_\nabla)^2 + (\eta^n_\delta)^2 + \left(\eta^n_f\right)^2 \right] + 7 \int_{t^{n-1}}^{t^n} \left\| \sqrt{\kappa} \nabla e \right\|^2_0 \mathrm{d}t\,. \tag{3.12}$$

Proof. Let us observe that

$$\int_{t^{n-1}}^{t^n}\left\langle\frac{\partial\, e(t)}{\partial t},v(t)\right\rangle+(\kappa\,\nabla\, e(t),\nabla v(t))\mathrm{d}t=\sum_{T_*,k_{T_*}}\int_{t^{k_{T_*}-1}}^{t^{k_{T_*}}}\left(R_{T_*}^{k_{T_*}},v(t)-I_h^n\,v(t)\right)_{T_*}\mathrm{d}t$$
$$+\sum_{E_*,k_{E_*}}\int_{t^{k_{E_*}-1}}^{t^{k_{E_*}}}\left(J_{E_*}^{k_{E_*}},\gamma_{E_*}(v(t)-I_h^n\,v(t))\right)_{E_*}\mathrm{d}t+\int_{t^{n-1}}^{t^n}r_\Omega^n(I_h^n\,v(t))\mathrm{d}t$$
$$-\int_{t^{n-1}}^{t^n}(f-\Pi_h^n\,f,v(t))\mathrm{d}t+\sum_{T_*,k_{T_*}}\int_{t^{k_{T_*}-1}}^{t^{k_{T_*}}}\left(\kappa\nabla\left[u_{h,\Delta t}(t)-\mathcal{M}^{k_{T_*}}(u_{h,\Delta t})\right],\nabla v(t)\right)_{T_*}\mathrm{d}t$$
$$-\int_{t^{n-1}}^{t^n}\left(\Pi_h^n\,f(t)-\sum_{T_*,k_{T_*}}\mathcal{M}^{k_{T_*}}(f_{h,\Delta t})\,\chi_{T_*}\,\chi_{k_{T_*}}(t),v(t)\right)\mathrm{d}t,$$

obtained by adding and removing $\int_{t^{n-1}}^{t^n}r_\Omega^n(I_h^n\,v)\mathrm{d}t$ to the left-hand side. Moreover, we consider that

$$\sqrt{\int_{t^{n-1}}^{t^n}\left\|\frac{\partial\, e}{\partial t}\right\|_{\kappa,-1}^2\mathrm{d}t}=\sup_{v\in\mathrm{L}^2(I^n,\mathrm{H}_0^1(\Omega))}\frac{\displaystyle\int_{t^{n-1}}^{t^n}\left\langle\frac{\partial\, e(t)}{\partial t},v(t)\right\rangle\mathrm{d}t}{\sqrt{\int_{t^{n-1}}^{t^n}\|\,v(t)\,\|_{\kappa,1}^2\mathrm{d}t}}.$$

Applying Hölder's inequality and Lemma 3.5 we get

$$\sqrt{\int_{t^{n-1}}^{t^n}\left\|\frac{\partial\, e}{\partial t}\right\|_{\kappa,-1}^2\mathrm{d}t}\le\eta_f^n+\eta_\nabla^n+\eta_\delta^n+Cl_R\sqrt{\sum_{T_*,k_{T_*}}\Delta t_{T_*}\left(h_{T_*}^{n-1,n}\right)^2\left\|\frac{1}{\sqrt{\kappa_{T_*}}}\,R_{T_*}^{k_{T_*}}\right\|_{0,T^*}^2}$$
$$+Cl_E\sqrt{\sum_{E_*,k_{E_*}}\Delta t_{E_*}\,h_{E_*}^{n-1,n}\left\|\,J_{E_*}^{k_{E_*}}\,/\,\sqrt{\hat\kappa_{\omega_{E_*}^n}}\right\|_{0,E^*}^2}+\sqrt{\int_{t^{n-1}}^{t^n}\|\,\sqrt{\kappa}\,\nabla\, e\,\|_0^2\mathrm{d}t}.$$

To get the thesis we square the previous relation and we consider that $(\sum_{i=1,\dots,m}a_i)^2\le m\sum_{i=1,\dots,m}a_i^2\ \forall a_i>0,\ i=1,\dots,m.$ ∎

COROLLARY 3.16. *Under the hypotheses of Theorems* 3.14 *and* 3.15*, there exist constants $C_{n-1}^{\uparrow,n}$, independent of any meshsize, timestep, and problem-parameter, but depending on the smallest angle of triangulations $\mathcal{T}_h^n$ and on the constant C_{tr}, such that the following inequality holds true for $n=1,\dots,N$:*

$$8\,\|\,e(t^n)\,\|_0^2+|\!|\!|\,e\,|\!|\!|_{\kappa,I^n}^2$$
$$\le 8\left\|\,e(t^{n-1})\,\right\|_0^2+C_{n-1}^{\uparrow,n}\left[(\eta_R^n)^2+(\eta_\nabla^n)^2+(\eta_\delta^n)^2+\left(\eta_f^n\right)^2\right],\tag{3.13}$$
$$8\,\|\,e(t^m)\,\|_0^2+|\!|\!|\,e\,|\!|\!|_{\kappa,(0,t^m)}^2\le 8\left\|\,e(t^0)\,\right\|_0^2$$
$$+C_0^{\uparrow,N}\sum_{n=1}^m\left[(\eta_R^n)^2+(\eta_\nabla^n)^2+(\eta_\delta^n)^2+\left(\eta_f^n\right)^2\right]\quad\forall m=1,\dots,N,\tag{3.14}$$

where $C_0^{\uparrow,N}=\max_{n=1,\dots,N}C_{n-1}^{\uparrow,n}$.

Proof. Multiplying inequality (3.8) by 8 and summing to (3.12), we get (3.13). ∎

3.3. Lower bound. In this section we prove that the terms η_R^n, η_∇^n, and η_δ^n bound from below the error of the discrete solution with respect to the exact solution of the continuous variational formulation. We consider separately the contribution of the equation residual, the interelement jumps, η_∇^n and η_δ^n.

3.3.1. Equation residual. Here we show how the residual of the equation can bound the error from below on the time interval I^n. Let us define the following functions:

$$w_{R,T_*}^{k_{T_*}}(x,t) = \left(h_{T_*}^{n-1,n}\right)^2 \frac{1}{\sqrt{\kappa_{T_*}}} R_{T_*}^{k_{T_*}}\, b_{T_*}(x)\, \chi_{k_{T_*}}(t) \quad \forall\, T_* \in \mathcal{T}_h^{n-1,n},\ k_{T_*} = 1,\dots,2^{J_{T_*}},$$

$$w_{R,\Omega}^n = \sum_{T_*,k_{T_*}} w_{R,T_*}^{k_{T_*}}\,.$$

If we admit different polynomial degrees of the finite element space for each timeslab, we assume an upper bound for it and this upper bound affects the constants in Lemmas 3.17 and 3.19 [18].

LEMMA 3.17. *There exist constants C_R and C_R^* independent of any meshsize, timestep, and problem-parameter such that*

$$h_{T_*}^{n-1,n^2} \left\| \frac{1}{\sqrt{\kappa_{T_*}}} R_{T_*}^{k_{T_*}} \right\|_{0,T_*}^2 \le C_R \left(\frac{1}{\sqrt{\kappa_{T_*}}} R_{T_*}^{k_{T_*}}, w_{R,T_*}^{k_{T_*}} \right)_{T_*}, \tag{3.15}$$

$$\left\| \nabla\, w_{R,T_*}^{k_{T_*}} \right\|_{0,T_*} \le C_R^*\, h_{T_*}^{n-1,n} \left\| \frac{1}{\sqrt{\kappa_{T_*}}} R_{T_*}^{k_{T_*}} \right\|_{0,T_*}. \tag{3.16}$$

Proof. These results come by exploiting the properties of bubble functions and the finite dimensionality of the residual function [17, 18]. □

PROPOSITION 3.18. *Under the assumptions on the continuous problem* (2.4) *and on the discrete formulation* (2.13)*, on each time interval $\left(t^{n-1}, t^n\right)$ we have*

$$\sqrt{\sum_{T_*,k_{T_*}} \left(h_{T_*}^{n-1,n}\right)^2 \left\| \frac{1}{\sqrt{\kappa_{T_*}}} R_{T_*}^{k_{T_*}} \right\|_{0,T_*}^2 \Delta t_{T_*}} \le 2 C_R C_R^* \left[\| e \|_{\kappa,I^n}^2 + \left(\eta_f^n\right)^2 \right]^{\frac{1}{2}}. \tag{3.17}$$

Proof. We start by subtracting from $\sum_{T_*,k_{T_*}} \int_{t^{k_{T_*}-1}}^{t^{k_{T_*}}} (R_{T_*}^{k_{T_*}} / \sqrt{\kappa_{T_*}}, w_{R,T_*}^{k_{T_*}})_{T_*}\, \mathrm{d}t$ the continuous variational formulation (2.4) with $w_{R,\Omega}^n / \sqrt{\kappa}$ as test function and integrate on the time interval I^n,

$$\begin{aligned}
\sum_{T_*,k_{T_*}} \int_{t^{k_{T_*}-1}}^{t^{k_{T_*}}} \left(\frac{1}{\sqrt{\kappa_{T_*}}} R_{T_*}^{k_{T_*}}, w_{R,T_*}^{k_{T_*}} \right)_{T_*} \mathrm{d}t &= \int_{t^{n-1}}^{t^n} \left\langle \frac{1}{\sqrt{\kappa}} \frac{\partial e}{\partial t}, w_{R,\Omega}^n \right\rangle \mathrm{d}t \\
&\quad - \sum_{T_*,k_{T_*}} \int_{t^{k_{T_*}-1}}^{t^{k_{T_*}}} \left(\sqrt{\kappa_{T_*}} \left[u_{h,\Delta t} - \mathcal{M}^{k_{T_*}}(u_{h,\Delta t}) \right], \nabla\, w_{R,T_*}^{k_{T_*}} \right)_{T_*} \mathrm{d}t \\
&\quad + \int_{t^{n-1}}^{t^n} \left(\frac{1}{\sqrt{\kappa}} \nabla\, e(t), \nabla\, w_{R,\Omega}^n \right) \mathrm{d}t + \int_{t^{n-1}}^{t^n} \left(\frac{1}{\sqrt{\kappa}} \left[f(t) - \Pi_h^n f(t) \right], w_{R,\Omega}^n \right) \mathrm{d}t \\
&\quad + \int_{t^{n-1}}^{t^n} \left(\frac{1}{\sqrt{\kappa}} \left[\Pi_h^n f(t) - \sum_{T_*,k_{T_*}} \mathcal{M}^{k_{T_*}}(f_{h,\Delta t})\, \chi_{T_*} \chi_{k_{T_*}}(t) \right], w_{R,\Omega}^n \right) \mathrm{d}t\,.
\end{aligned}$$

Applying Cauchy–Schwarz and Hölder inequalities, observing that $w_{R,T_*}^{k_{T_*}}$ is a constant function on the interval $\left(t^{k_{T_*}-1}, t^{k_{T_*}}\right)$, that $\int_{t^{k_{T_*}-1}}^{t^{k_{T_*}}} [\frac{t-t^{k_{T_*}-1}}{t^{k_{T_*}}-t^{k_{T_*}-1}} - \frac{1}{2}]\,\mathrm{d}t = 0$, and using inequalities (3.15)–(3.16) we get the thesis. ∎

3.3.2. Interelement jumps. Now we consider the edges $E_* \in \mathcal{E}_{h,\Omega}^{n-1,n}$ and we show how the jumps $J_{E_*}^{k_{E_*}}$ can bound the error from below. Let us define

$$w_{J,E_*}^{k_{E_*}}(x,t) = h_{E_*}^{n-1,n}\,\mathcal{P}_E\left(\frac{1}{\sqrt{\hat{\kappa}_{\omega_{E_*}^n}}}\,J_{E_*}^{k_{E_*}}\right) b_{E_*}(x)\,\chi_{k_{E_*}}(t)\ \forall\, E_* \in \mathcal{E}_{h,\Omega}^{n-1,n},\ k_{E_*} = 1,\dots,2^{J_{E_*}}.$$

We remark that $w_{J,E_*}^{k_{E_*}}$ vanishes on the edges of the elements $T' \in \mathcal{T}_{h,\mathring{\omega}}^{n-1,n}$ inside the elements $T_* \in \mathcal{T}_h^{n-1,n}$.

Let us assume a local substepping regularity partition property for the nodes of neighboring triangles: there exists a constant σ_{E_*} such that $J_{E_*} - J_{T'} \le \sigma_{E_*}\ \forall T' \in \mathring{\omega}_{E_*}^n$.

Thanks to the orthogonality of our system of edge-bubble functions, we have

$$\left\| \sum_{E_*,k_{E_*}} \nabla\, w_{J,E_*}^{k_{E_*}} \right\|_0^2 = \sum_{E_*,k_{E_*}} \left\| \nabla\, w_{J,E_*}^{k_{E_*}} \right\|_{0,\mathring{\omega}_{E_*}^n}^2 .$$

LEMMA 3.19. *There exist constants C_E and C_E^* independent of any meshsize, timestep, and problem-parameter such that*

$$h_{E_*}^{n-1,n} \left\| J_{E_*}^{k_{E_*}} / \sqrt{\hat{\kappa}_{\omega_{E_*}^n}} \right\|_{0,E_*}^2 \le C_E \left(J_{E_*}^{k_{E_*}} / \sqrt{\hat{\kappa}_{\omega_{E_*}^n}}, w_{J,E_*}^{k_{E_*}} \right)_{E_*}, \tag{3.18}$$

$$\left\| \nabla\, w_{J,E_*}^{k_{E_*}} \right\|_{0,\mathring{\omega}_{E_*}^n} \le C_E^* \sqrt{h_{E_*}^{n-1,n}} \left\| J_{E_*}^{k_{E_*}} / \sqrt{\hat{\kappa}_{\omega_{E_*}^n}} \right\|_{0,E_*} . \tag{3.19}$$

Proof. The inequalities (3.18)–(3.19) are derived by exploiting the properties of bubble functions and inverse inequalities for the jump functions [17, 18]. ∎

LEMMA 3.20. *There exist constants $C_{\mathring{\omega}_{E_*}^n}$ and C_{reg} independent of any meshsize, timestep, and problem-parameter, but depending on the maximum of σ_{E_*} over all the edges $E_* \in \mathcal{E}_{h,\Omega}^{n-1,n}$ and on the regularity of the mesh $\mathcal{T}_h^{n-1,n}$, respectively, such that*

$$\begin{aligned} &\sum_{E_*,k_{E_*}} \sum_{T' \in \mathring{\omega}_{E_*}^n} \left(h_{E_*}^{n-1,n}\right)^2 \left\| \frac{1}{\sqrt{\kappa_{T'}}}\, R_{T'}^{k_{E_*}} \right\|_{0,T'}^2 \Delta t_{E_*} \\ &\qquad \le C_{\mathring{\omega}_{E_*}^n}\, C_{reg} \sum_{T_*,k_{T_*}} \left(h_{T_*}^{n-1,n}\right)^2 \left\| \frac{1}{\sqrt{\kappa_{T'}}}\, R_{T_*}^{k_{T_*}} \right\|_{0,T_*}^2 \Delta t_{T_*} . \end{aligned} \tag{3.20}$$

Proof. Inequality (3.20) follows from the local regularity hypothesis for the mesh $\mathcal{T}_h^{n-1,n}$, from the local regularity of the substepping partition for the nodes of neighboring triangles, and from $\Delta t_{T'} = \Delta t_{T_*}\ \forall T' \in T_*$. ∎

PROPOSITION 3.21. *Under the assumptions on the continuous problem* (2.4) *and*

on the discrete formulation (2.13)*, on each time interval* $\left(t^{n-1}, t^n\right)$ *we have*

$$\sqrt{\sum_{E_*, k_{E_*}} h_{E_*}^{n-1,n} \left\| \frac{1}{\sqrt{\hat{\kappa}_{\omega_{E_*}^n}}} J_{E_*}^{k_{E_*}} \right\|_{0,E_*}^2 \Delta t_{E_*}} \leq 2C_E \left(C_E^* + C_R C_R^* C_{reg}\right) \times \sqrt{\| e \|_{\kappa, I^n}^2 + \left(\eta_f^n\right)^2}. \tag{3.21}$$

Proof. We start by subtracting the continuous variational formulation (2.4) to the quantity $(\sum_{E_*, k_{E_*}} J_{E_*}^{k_{E_*}} / \sqrt{\hat{\kappa}_{\omega_{E_*}^n}}, \sum_{E_*, k_{E_*}} w_{J,E_*}^n)$ and integrating in time over I^n,

$$\begin{aligned}
&\sum_{E_*, k_{E_*}} \int_{t^{k_{E_*}-1}}^{t^{k_{E_*}}} \left(\frac{1}{\sqrt{\hat{\kappa}_{\omega_{E_*}^n}}} J_{E_*}^{k_{E_*}}, w_{J,E_*}^{k_{E_*}} \right)_{E_*} \mathrm{d}t \\
&\quad = \int_{t^{n-1}}^{t^n} \left\langle \frac{\partial e}{\partial t}, \sum_{E_*, k_{E_*}} \frac{1}{\sqrt{\hat{\kappa}_{\omega_{E_*}^n}}} w_{J,E_*}^{k_{E_*}} \right\rangle \mathrm{d}t \\
&\qquad + \int_{t^{n-1}}^{t^n} \left(\nabla e, \sum_{E_*, k_{E_*}} \frac{\kappa}{\sqrt{\hat{\kappa}_{\omega_{E_*}^n}}} \nabla w_{J,E_*}^{k_{E_*}} \right) \mathrm{d}t \\
&\qquad + \int_{t^{n-1}}^{t^n} \left(f - \Pi_h^n f, \sum_{E_*, k_{E_*}} \frac{1}{\sqrt{\hat{\kappa}_{\omega_{E_*}^n}}} w_{J,E_*}^{k_{E_*}} \right) \mathrm{d}t \\
&\qquad + \int_{t^{n-1}}^{t^n} \left(\Pi_h^n f - \sum_{T_*, k_{T_*}} \mathcal{M}^{k_{T_*}}(f_{h,\Delta t}) \chi_{T_*} \chi_{k_{T_*}}(t), \sum_{E_*, k_{E_*}} \frac{1}{\sqrt{\hat{\kappa}_{\omega_{E_*}^n}}} w_{J,E_*}^n \right) \mathrm{d}t \\
&\qquad - \sum_{E_*, k_{E_*}} \sum_{T' \in \mathring{\omega}_{E_*}^n} \int_{t^{k_{E_*}-1}}^{t^{k_{E_*}}} \left(\frac{1}{\sqrt{\hat{\kappa}_{\omega_{E_*}^n}}} R_{T'}^{k_{E_*}}, w_{J,E_*}^{k_{E_*}} \right)_{T'} \mathrm{d}t \\
&\qquad - \sum_{E_*, k_{E_*}} \int_{t^{k_{E_*}-1}}^{t^{k_{E_*}}} \left[\frac{t - t^{k_{E_*}-1}}{t^{k_{E_*}} - t^{k_{E_*}-1}} - \frac{1}{2} \right] \\
&\qquad \times \sum_{T' \in \mathring{\omega}_{E_*}^n} \left(\nabla \left(u_{h,\Delta t}(t^{k_{E_*}}) - u_{h,\Delta t}(t^{k_{E_*}-1}) \right), \sum_{E_* \in \mathcal{E}_{h,\Omega}^{n-1,n}} \frac{\kappa}{\sqrt{\hat{\kappa}_{\omega_{E_*}^n}}} \nabla w_{J,E_*}^n \right)_{T'} \mathrm{d}t.
\end{aligned}$$

Then we apply Cauchy–Schwarz and Hölder inequalities, inequality (3.19), orthogonality of the edge-bubble functions, and inequalities (3.18), (3.20), and (3.17) to obtain (3.21). ∎

3.3.3. Time discretization estimator. Now we show how the term η_∇^n can bound the error from below. Let us define

$$w_{\nabla,T_*}^{k_{T_*}}(x) = \left[\frac{t - t^{k_{T_*}-1}}{t^{k_{T_*}} - t^{k_{T_*}-1}} - \frac{1}{2}\right]\left(u_{h,\Delta t}(t^{k_{T_*}}) - u_{h,\Delta t}(t^{k_{T_*}-1})\right)\chi_{T_*}\,\chi_{k_{T_*}}(t),$$

$$w_{\nabla,\Omega}^n = \sum_{T_*\in\mathcal{T}_h^{n-1,n}}\sum_{k_{T_*}=1}^{2^{J_{T_*}}} w_{\nabla,T_*}^{k_{T_*}}\,.$$

PROPOSITION 3.22. *Under the assumptions on the continuous problem* (2.4) *and on the discrete formulation* (2.13)*, on each time interval* $\left(t^{n-1},t^n\right)$ *the inequality*

$$\eta_\nabla^n \le 2\sqrt{\|\!|\, e \,|\!\|_{\kappa,I^n}^2 + \left(\eta_f^n\right)^2} \tag{3.22}$$

holds true.

Proof. We start by observing that $\forall t \in (t^{k_{T_*}-1}, t^{k_{T_*}})$,

$$\begin{aligned}\left(\eta_{\nabla,T_*}^{k_{T_*}}\right)^2 &= \int_{t^{k_{T_*}-1}}^{t^{k_{T_*}}}\left(\kappa\nabla\left(u_{h,\Delta t} - \mathcal{M}^{k_{T_*}}(u_{h,\Delta t})\right),\nabla w_{\nabla,T_*}^{k_{T_*}}\right)_{T_*}\mathrm{d}t\\ &= \int_{t^{k_{T_*}-1}}^{t^{k_{T_*}}}\left[\frac{t - t^{k_{T_*}-1}}{t^{k_{T_*}} - t^{k_{T_*}-1}} - \frac{1}{2}\right]\left(\kappa\nabla\left(u_{h,\Delta t}(t^{k_{T_*}}) - u_{h,\Delta t}(t^{k_{T_*}-1})\right),\nabla\, w_{\nabla,T_*}^{k_{T_*}}\right)_{T_*}\mathrm{d}t\end{aligned}$$

and remarking that $\int_{t^{k_{T_*}-1}}^{t^{k_{T_*}}}(w, w_{\nabla,T_*}^{k_{T_*}})_{T_*}\,\mathrm{d}t = 0$ for any function w constant in time in each time interval $(t^{k_{T_*}-1}, t^{k_{T_*}})$ on each element $T_* \in \mathcal{T}_h^{n-1,n}$. In the following we apply this property by taking $w = \kappa\,\nabla\,\mathcal{M}^{k_{T_*}}(u_{h,\Delta t})$, obtaining

$$\left(\eta_{\nabla,T_*}^{k_{T_*}}\right)^2 = \int_{t^{k_{T_*}-1}}^{t^{k_{T_*}}}\left(\kappa\nabla u_{h,\Delta t},\nabla w_{\nabla,T_*}^{k_{T_*}}\right)_{T_*}\mathrm{d}t,$$

and then again with $w = \frac{\partial\, u_{h,\Delta t}}{\partial t}$ and $w = -\,\mathcal{M}^{k_{T_*}}(f_{h,\Delta t})$. Summing over all $T_* \in \mathcal{T}_h^{n-1,n}$ and $k_{T_*} = 1,\dots,2^{J_{T_*}}$, subtracting (2.4) we get

$$\sum_{T_*,k_{T_*}}\left(\eta_{\nabla,T_*}^{k_{T_*}}\right)^2 = \int_{t^{n-1}}^{t^n}\left\langle\frac{\partial\, e}{\partial t}, w_{\nabla,\Omega}^n\right\rangle\mathrm{d}t + \int_{t^{n-1}}^{t^n}\left(\kappa\,\nabla\, e, \nabla\, w_{\nabla,\Omega}^n\right)\mathrm{d}t$$

$$+\int_{t^{n-1}}^{t^n}\left(f - \Pi_h^n f, w_{\nabla,\Omega}^n\right)\mathrm{d}t + \int_{t^{n-1}}^{t^n}\left(\Pi_h^n f - \sum_{T_*,k_{T_*}}\mathcal{M}^{k_{T_*}}(f_{h,\Delta t})\,\chi_{T_*}\,\chi_{k_{T_*}}(t), w_{\nabla,\Omega}^n\right)\mathrm{d}t\,.$$

Applying Cauchy–Schwarz and Hölder inequalities, (3.22) follows. ∎

3.3.4. Level transition estimator. Now we show how the norm $\left(\eta_\delta^n\right)^2$ can bound the error from below.

PROPOSITION 3.23. *Under the assumptions on the continuous problem* (2.4) *and on the discrete formulation* (2.13)*, on each time interval* $\left(t^{n-1},t^n\right)$ *the inequality*

$$\eta_\delta^n \le \sqrt{\left(\eta_\nabla^n\right)^2} + 2\sqrt{\|\!|\, e \,|\!\|_{\kappa,I^n}^2 + \left(\eta_f^n\right)^2} \tag{3.23}$$

holds true.

Proof. We start by observing that

$$\eta_\delta^n = \sup_{v_h \in \mathrm{L}^2(I^n, \mathrm{V}_h^n)} \frac{1}{\sqrt{\int_{t^{n-1}}^{t^n} \| v_h \|_{\kappa,1}^2 \mathrm{d}t}} \left[\int_{t^{n-1}}^{t^n} r_\Omega^k(v_h) \mathrm{d}t - \int_{t^{n-1}}^{t^n} \left\langle \frac{\partial u}{\partial t}, v_h \right\rangle + (\kappa \nabla u, \nabla v_h) - (f, v_h) \mathrm{d}t \right].$$

Then, adding and subtracting the quantity $\int_{t^{n-1}}^{t^n} (\kappa \nabla u_{h,\Delta t}, \nabla v_h) + (\Pi_h^n f, v_h) \mathrm{d}t$, we get

$$\begin{aligned}\sqrt{\int_{t^{n-1}}^{t^n} \|r_\Omega^n\|_{\kappa,-1,\mathcal{T}_h}^2 \mathrm{d}t} = \sup_{v_h \in \mathrm{L}^2(I^n, \mathrm{V}_h^n)} \frac{1}{\sqrt{\int_{t^{n-1}}^{t^n} \| v_h \|_{\kappa,1}^2 \mathrm{d}t}} \Bigg[& \int_{t^{n-1}}^{t^n} \left(\frac{\partial e}{\partial t}, v_h \right) \mathrm{d}t \\ & + \int_{t^{n-1}}^{t^n} (\kappa \nabla e, \nabla v_h) \mathrm{d}t + \int_{t^{n-1}}^{t^n} (f - \Pi_h^n f, v_h) \mathrm{d}t \\ & + \int_{t^{n-1}}^{t^n} \left(\Pi_h^n f - \sum_{T_*, k_{T_*}} \mathcal{M}^{k_{T_*}}(f_{h,\Delta t}) \, \chi_{T_*} \, \chi_{k_{T_*}}(t), v_h \right) \mathrm{d}t \\ - \sum_{T_*, k_{T_*}} \int_{t^{k_{T_*}-1}}^{t^{k_{T_*}}} & \left[\frac{t - t^{k_{T_*}-1}}{t^{k_{T_*}} - t^{k_{T_*}-1}} - \frac{1}{2} \right] \left(\kappa \nabla \left(u_{h,\Delta t}(t^{k_{T_*}}) - u_{h,\Delta t}(t^{k_{T_*}-1}) \right), \nabla v_h \right)_{T_*} \mathrm{d}t \Bigg].\end{aligned}$$

Applying Cauchy–Schwarz and Hölder inequalities, the thesis easily follows. ∎

3.3.5. Final lower bounds. We are now in a position to state the final lower bounds in the following theorem. The result is a straightforward consequence of Propositions 3.18, 3.21, 3.22, and 3.23.

THEOREM 3.24. *Under the assumptions on the continuous problem* (2.4) *and on the discrete formulation* (2.13)*, there exist constants* $C_{\downarrow,n-1}^n$ *independent of any meshsize, timestep, and problem-parameter, but depending on the smallest angle of the triangulation* $\mathcal{T}_h^n$*, on* C_{tr}*, and on the upper bound of the polynomial degree of the finite element space used in each timeslab such that the following inequalities hold true:*

$$(\eta_R^n)^2 + (\eta_\nabla^n)^2 + (\eta_\delta^n)^2 \leq C_{\downarrow,n-1}^n \left(\| e \|_{\kappa,I^n}^2 + \left(\eta_f^n\right)^2 \right), \tag{3.24}$$

$$\sum_{n=1}^m \left((\eta_R^n)^2 + (\eta_\nabla^n)^2 + (\eta_\delta^n)^2 \right) \leq C_{\downarrow,0}^N \sum_{n=1}^m \left(\| e \|_{\kappa,I^n}^2 + \left(\eta_f^n\right)^2 \right) \tag{3.25}$$

$\forall m = 1, \ldots, N$*, where* $C_{\downarrow,0}^N = \max_{n=1,\ldots,N} C_{\downarrow,n-1}^n$.

4. Numerical tests.

4.1. Effectivity index and a posteriori estimators. This section aims at comparing the derived error estimators with the true error and investigating the behavior of the different error estimators. We define the following *effectivity index*:

$$e.i.^n = \frac{e.r.e^n}{t.r.e^n} = \frac{\sqrt{(\eta_R^n)^2 + (\eta_\nabla^n)^2 + (\eta_\delta^n)^2}}{\| e \|_{\kappa,I^n}}. \tag{4.1}$$

TABLE 1
Minimum and maximum effectivity index for $n = 1, \dots, N$.

J_p	$N = 4$	$N = 8$	$N = 16$	$N = 32$	$N = 64$	$N = 128$	$N = 256$
000	$0.9 - 1.7$	$0.3 - 2.1$	$0.8 - 4.1$	$2.4 - 8.3$	$2.6 - 10.0$	$3.4 - 10.0$	$3.4 - 8.2$
011	$0.8 - 1.8$	$1.8 - 3.2$	$3.0 - 6.8$	$4.2 - 10.0$	$3.5 - 9.9$	$3.4 - 8.2$	$3.4 - 5.3$
012	$1.8 - 2.7$	$3.3 - 6.3$	$6.4 - 9.9$	$3.8 - 9.9$	$3.5 - 8.1$	$3.4 - 5.3$	$3.4 - 4.0$
022	$1.8 - 2.8$	$3.3 - 6.3$	$6.4 - 9.9$	$3.8 - 9.9$	$3.5 - 8.1$	$3.4 - 5.3$	$3.4 - 4.0$
014	$6.1 - 7.7$	$6.3 - 8.6$	$4.0 - 7.0$	$3.5 - 5.0$	$3.4 - 4.0$	$3.4 - 3.6$	$3.4 - 3.5$
044	$6.8 - 9.0$	$6.6 - 8.9$	$3.9 - 7.0$	$3.5 - 5.0$	$3.4 - 4.0$	$3.4 - 3.6$	$3.4 - 3.5$
038	$3.7 - 4.1$	$3.6 - 3.9$	$3.5 - 3.9$	$3.5 - 3.7$	$3.4 - 3.5$	$3.4 - 3.5$	$3.4 - 3.4$
088	$3.6 - 3.7$	$3.5 - 3.5$	$3.5 - 3.5$	$3.4 - 3.5$	$3.4 - 3.4$	$3.4 - 3.4$	$3.4 - 3.4$

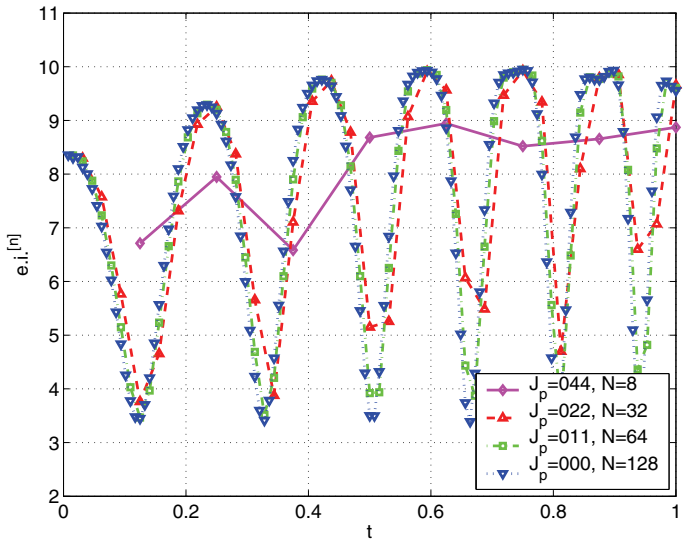

FIG. 8. *e.i.^{n} for several values of J_p and N.*

In our definition of the effectivity index we do not consider the effects of the data approximation errors η_f^n. We are mainly interested in the effects of the time-substeps, so we consider meshes fine enough to have a negligible error η_{f,Π_h}^n, whereas some of our results can be affected by the error $\eta_{f,\Delta t}^n$, and we shall highlight this phenomenon when it occurs.

We consider the same simple test problem of subsection 2.5 with the same space discretization, and we compare the true error with our error estimators for different timestep-lengths and substep-levels.

All the H^{-1}-norms are approximated by the solution of a Poisson problem in each substep of level $J = \max_{p \in \mathcal{N}_h^n(\overline{\Omega})} J_p^n$.

In Table 1 we report the effectivity indices (4.1) for several substepping configurations. The first row with $J_p = 0$ for all the three regions ($J_p = 000$) corresponds to the classical Crank–Nicolson scheme and $\eta_\delta^n = 0$. The following rows correspond to higher substep-levels in the two central regions. Each column reports the number of timesteps N and the corresponding minimum and maximum values of the effectivity index over all $n = 1, \dots, N$.

In Figure 8 we report the time evolution of the effectivity index for several values of J_p and N. In Figure 9 we display the behavior of the effectivity index for a fixed

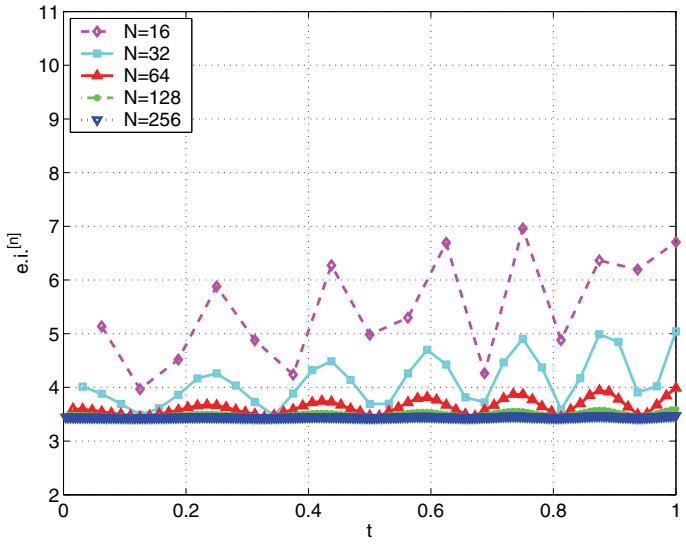

FIG. 9. *e.i.^{n} for $J_p = 014$ and several values of N.*

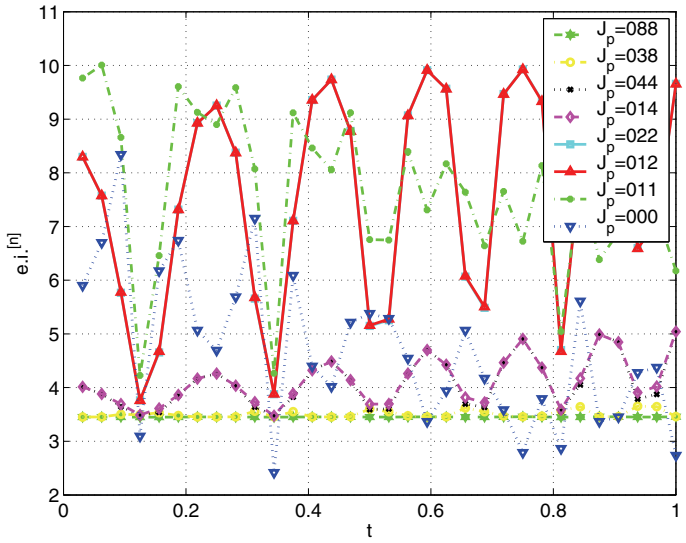

FIG. 10. *e.i.^{n} for $N = 32$ and several values of J_p.*

$J_p = 014$ and several N, and in Figure 10 for a fixed $N = 32$ and several J_p.

In Tables 2 and 3 we report the maximum values of the space data approximation error $\max_{n=1,\dots,N} \eta^n_{f,\Pi_h}$ and of the time data approximation error $\max_{n=1,\dots,N} \eta^n_{f,\Delta t}$, respectively. We remark that the error η^n_{f,Π_h} is independent of the substep levels, and for this reason we report just one row for all the substepping configurations. On the other hand, the error $\eta^n_{f,\Delta t}$ is strongly varying in the number of timesteps and substep-levels. We remark that the values of $\eta^n_{f,\Delta t}$ corresponding to the smallest number of timesteps and substep-levels are very large, and this explains the anomalous low values of the effectivity index in the corresponding cells of Table 1.

TABLE 2
Maximum η^n_{f,Π_h} for $n = 1, \dots, N$, the values are independent of the substep levels.

J_p	$N = 4$	$N = 8$	$N = 16$	$N = 32$	$N = 64$	$N = 128$	$N = 256$
0XY	0.00516	0.00363	0.0026	0.00184	0.0013	0.000923	0.000653

TABLE 3
Maximum $\eta^n_{f,\Delta t}$ for $n = 1, \dots, N$.

J_p	$N = 4$	$N = 8$	$N = 16$	$N = 32$	$N = 64$	$N = 128$	$N = 256$
000	3.13	2.37	1.39	0.671	0.251	0.0876	0.0307
011	3.09	1.65	0.813	0.327	0.121	0.0432	0.0153
012	2.26	0.988	0.393	0.158	0.0599	0.0215	0.00764
022	2.26	0.987	0.392	0.158	0.0599	0.0215	0.00764
014	0.657	0.244	0.116	0.0433	0.0166	0.00625	0.00228
044	0.65	0.234	0.0946	0.0391	0.0149	0.00538	0.00191
038	0.193	0.128	0.0832	0.0417	0.017	0.0063	0.00238
088	0.0391	0.0145	0.0059	0.00244	0.000931	0.000336	0.000119

TABLE 4
Maximum η^n_{∇} for $n = 1, \dots, N$.

J_p	$N = 4$	$N = 8$	$N = 16$	$N = 32$	$N = 64$	$N = 128$	$N = 256$
000	3.82	2.87	2.31	1.52	0.715	0.287	0.105
011	3.84	2.8	1.93	0.949	0.397	0.147	0.0526
012	3.78	2.28	1.19	0.519	0.203	0.074	0.0263
022	3.78	2.28	1.19	0.519	0.203	0.074	0.0263
014	1.98	0.781	0.323	0.133	0.0512	0.0185	0.00659
044	1.97	0.779	0.323	0.133	0.0512	0.0185	0.00659
038	0.145	0.0511	0.0203	0.00836	0.0032	0.00116	0.000412
088	0.135	0.0499	0.0203	0.00835	0.0032	0.00116	0.000412

TABLE 5
Maximum η^n_{δ} for $n = 1, \dots, N$.

J_p	$N = 4$	$N = 8$	$N = 16$	$N = 32$	$N = 64$	$N = 128$	$N = 256$
000	0.0	0.0	0.0	0.0	0.0	0.0	0.0
011	0.0316	0.0151	0.00426	0.000222	$1.6e-05$	$3.08e-06$	$1.76e-06$
012	0.132	0.0859	0.0402	0.0227	0.00865	0.00338	0.00123
022	0.0204	0.00488	0.000939	$5.49e-05$	$7.93e-06$	$2.82e-06$	$2.52e-06$
014	0.129	0.102	0.0749	0.0384	0.0153	0.00575	0.00216
044	0.00157	0.000303	$6.2e-05$	$1.04e-05$	$8.28e-06$	$3.67e-06$	$2.74e-06$
038	0.189	0.128	0.0829	0.0415	0.0169	0.00629	0.00238
088	$2.23e-05$	$1.72e-05$	$1.07e-05$	$1.06e-05$	$8.31e-06$	$3.7e-06$	$2.76e-06$

In Table 4 we report the largest values of η^n_{∇} on the time interval of the simulation. We can observe a very large variation of these values with the number of timesteps and substep-levels. For small numbers of timesteps and substep-levels the time error estimator is larger than the space error estimator, which means that a refinement of the time discretization is required. For large values of timestep and substep-levels, the time discretization error becomes negligible with respect to the space discretization error.

In Table 5 we report the largest values of η^n_{δ}. We remark that this value is zero for the classical Crank–Nicolson scheme. For a fixed number of timesteps N, we point out some strong variations of these values. These strong variations mainly occur when, close to the region presenting fast changes in the solution, we have a jump of the

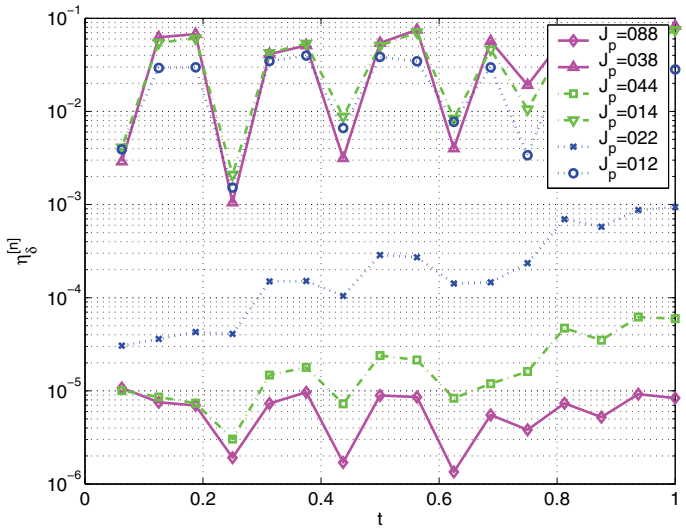

FIG. 11. *Evolution of η_δ^n with and without a level transition at the nodes x_1, x_2, x_3, and x_4, $N = 16$.*

corresponding substep-levels: compare, for example, the values of η_δ^n for $J_p = 012$ with 022, and $J_p = 014$ with 044, and $J_p = 038$ with 088. This behavior confirms the role of η_δ^n as a transition error estimator and suggests moving the jumps of substep-levels as far as possible from the regions with strong variations of the solution. Finally, Figure 11 compares the behavior of η_δ^n for $N = 16$ when a level transition is placed at the nodes x_1, x_2, x_3, and x_4 and when the transition is placed only at x_1 and x_2.

4.2. Approximation of η_δ^n. Our error estimator is composed of five different terms. In Remark 3.12 we already described the meaning of these terms.

Particular attention has to be paid when dealing with the term η_δ^n. This term, indeed, involves a discrete H^{-1}-norm of a functional that is constant in each of the 2^J substep of level J, and can be approximated through additional computations.

In what follows we propose a strategy for obtaining an upper and a lower approximate bound for η_δ^n at a moderate computational effort. From the definition of $r_\Omega^n(v_h)$ given in (3.7), Definition 3.10, and Remark 3.13, applying Hölder, trace, and inverse inequalities $\forall k = 1, \dots, 2^J$, we can write $r_\Omega^k(v_h) \precsim \| r_\Omega^k \|_0 \| v_h \|_{0,\Omega_{h,tr}^n}$ with

$$\| r_\Omega^k \|_0 = \sqrt{\sum_{T_* \in \mathcal{T}_{h,tr}^{n-1,n}} \left\| R_{T_*}^k \right\|_{0,T_*}^2} + \sqrt{\sum_{E_* \in \mathcal{E}_{h,tr,\Omega_{h,tr}^n}^{n-1,n}} \frac{1}{h_{E_*}^{n-1,n}} \| J_{E_*}^k \|_{0,E_*}^2},$$

where $\Omega_{h,tr}^n \subset \Omega$ is the domain corresponding to the partition $\mathcal{T}_{h,tr}^n$, and $\mathcal{E}_{h,tr,\Omega_{h,tr}^n}^{n-1,n}$ is the set of the internal edges of the partition $\mathcal{T}_{h,tr}^n$ contained in $\Omega_{h,tr}^n$.

We then look for the indices k for which $\| r_\Omega^k \|_0$ attains its minimum and maximum values: we call such indices k_{min} and k_{max}, respectively. We then approximate the discrete H^{-1}-norm $\left\| r_\Omega^k \right\|_{\kappa,-1,\mathcal{T}_h}$ for $k = k_{min}$, $k = k_{mid} = 2^{J-1}$, and $k = k_{max}$ by solving the following problem: *find* $r_h \in \mathrm{V}_h^n$ *such that* $\left(\kappa \nabla r_h^k, \nabla v_h\right) = r_\Omega^k(v_h)$

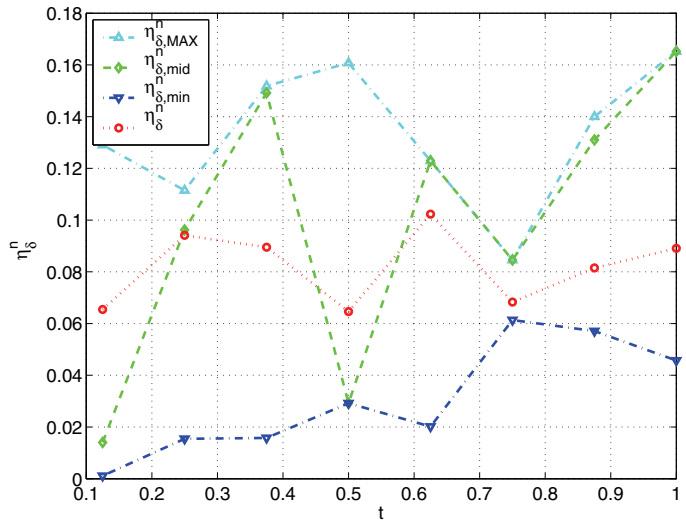

FIG. 12. η^n_δ, $\eta^n_{\delta,min}$, $\eta^n_{\delta,mid}$, $\eta^n_{\delta,max}$ *for* $J_p = 014$ *and* $N = 8$.

$\forall v_h \in \mathrm{V}^n_h$. We set $\left\|r^k_\Omega\right\|^2_{\kappa,-1,\mathcal{T}_h} = \left\|r^k_h\right\|^2_{\kappa,1}$. Then we propose using

$$\left(\eta^n_{\delta,max}\right)^2 = \Delta t^n \max\left\{\left\|r^{k_{min}}_\Omega\right\|^2_{\kappa,-1,\mathcal{T}_h}, \left\|r^{k_{mid}}_\Omega\right\|^2_{\kappa,-1,\mathcal{T}_h}, \left\|r^{k_{max}}_\Omega\right\|^2_{\kappa,-1,\mathcal{T}_h}\right\}$$

as the upper bound for $\left(\eta^n_\delta\right)^2$ and

$$\left(\eta^n_{\delta,min}\right)^2 = \Delta t^n \min\left\{\left\|r^{k_{min}}_\Omega\right\|^2_{\kappa,-1,\mathcal{T}_h}, \left\|r^{k_{mid}}_\Omega\right\|^2_{\kappa,-1,\mathcal{T}_h}, \left\|r^{k_{max}}_\Omega\right\|^2_{\kappa,-1,\mathcal{T}_h}\right\}$$

as the lower bound for $\left(\eta^n_\delta\right)^2$. We also define $\left(\eta^n_{\delta,mid}\right)^2 = \Delta t^n \left\|r^{k_{mid}}_\Omega\right\|^2_{\kappa,-1,\mathcal{T}_h}$.

Being the term η^n_δ related to the transition of the levels of the nodes in some elements, when it is large this suggests that the region with higher values of J^n_T should be enlarged toward the elements with smaller values of J^n_T, moving the level-transition on elements with smaller errors. Otherwise, if it is very small, this suggests reducing the regions with larger levels J^n_T.

Figure 12 displays the behavior of η^n_δ, $\eta^n_{\delta,min}$, $\eta^n_{\delta,mid}$, and $\eta^n_{\delta,max}$ for $N = 8$ and $J_p = 014$. In this picture we can see that $\eta^n_{\delta,mid}$ is a good approximation of η^n_δ and that $\eta^n_{\delta,min}$ and $\eta^n_{\delta,max}$ correctly bound η^n_δ. Figure 13 displays the behavior of effectivity index using $\eta^n_{\delta,min}$, $\eta^n_{\delta,mid}$, and $\eta^n_{\delta,max}$ for its computation instead of η^n_δ, we can observe very small differences.

5. Conclusions. We have proposed a new discretization method for the heat equation that allows the coexistence of short and long timesteps on different elements. We proved existence and uniqueness of the numerical solution, and provided a stability estimate and a posteriori upper and lower residual-based error estimators for this new method. Moreover, we report a numerical example that shows the possible gain in efficiency offered by the substepped method and some comparisons between the true error and the derived a posteriori error estimators.

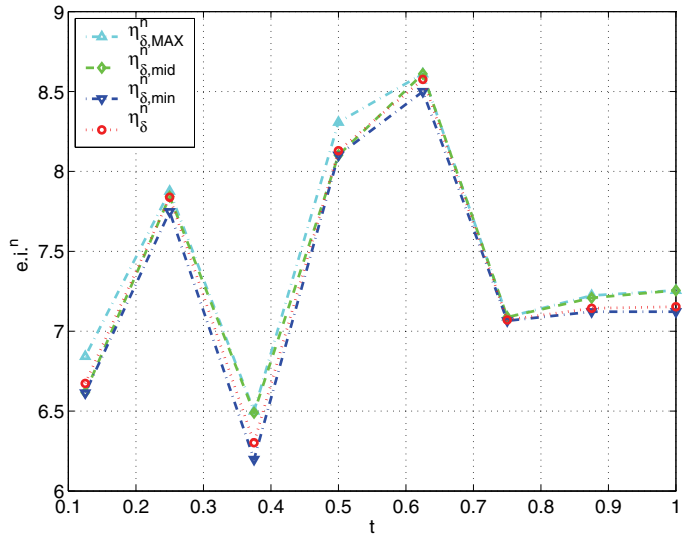

FIG. 13. *e.i.^{n} computed using the exact value of η^n_δ, $\eta^n_{\delta,min}$, $\eta^n_{\delta,mid}$, $\eta^n_{\delta,max}$ for $J_p = 014$ and $N = 8$.*

In this work an attempt was not made to address the complex problem of the set up of an adaptive algorithm based on the upper and lower robust estimates derived in section 3. This will be dealt with in a future investigation.

REFERENCES

[1] G. AKRIVIS, C. MAKRIDAKIS, AND R. H. NOCHETTO, *A posteriori error estimates for the Crank-Nicolson method for parabolic equations*, Math. Comp., 75 (2006), pp. 511–531.

[2] I. BABUŠKA AND W. C. RHEINBOLDT, *Error estimates for adaptive finite element method*, SIAM J. Numer. Anal., 15 (1978), pp. 736–754.

[3] R. BECKER AND R. RANNACHER, *An optimal control approach to a posteriori error estimation in finite element methods*, Acta Numer., 10 (2001), pp. 1–102.

[4] A. BERGAM, C. BERNARDI, AND Z. MGHAZLI, *A posteriori analysis of the finite element discretization of some parabolic equations*, Math. Comp., 74 (2005), pp. 1117–1138.

[5] C. BERNARDI AND R. VERFÜRTH, *Adaptive finite element methods for elliptic equations with non-smooth coefficients*, Numer. Math., 85 (2000), pp. 579–608.

[6] S. BERRONE, *Robust a posteriori error estimates for finite element discretizations of the heat equation with discontinuous coefficients*, M2AN Math. Model. Numer. Anal., 40 (2006), pp. 991–1021.

[7] P. BINEV, W. DAHMEN, AND R. DEVORE, *Adaptive finite element methods with convergence rates*, Numer. Math., 97 (2004), pp. 219–268.

[8] P. G. CIARLET, *The Finite Element Method for Elliptic Problems*, North–Holland Publishing Co., Amsterdam, 1978.

[9] PH. CLÉMENT, *Approximation by finite element functions using local regularization*, Rev. Franc. Automat. Inform. Rech. Operat., 9 (1975), pp. 77–84.

[10] W. DÖRFLER, *A convergent adaptive algorithm for Poisson's equation*, SIAM J. Numer. Anal., 33 (1996), pp. 1106–1124.

[11] M. DRYJA, M. V. SARKIS, AND O. B. WIDLUND, *Multilevel Schwarz methods for elliptic problems with discontinuous coefficients in three dimensions*, Numer. Math., 72 (1996), pp. 313–348.

[12] K. ERIKSSON, D. ESTEP, P. HANSBO, AND C. JOHNSON, *Introduction to adaptive methods for differential equations*, A. Isertes, ed., Acta Numerica, Cambridge University Press, Cambridge, UK, 1995, pp. 105–158.

[13] P. MORIN, R. H. NOCHETTO, AND K. G. SIEBERT, *Convergence of adaptive finite element*

methods, SIAM Rev., 44 (2002), pp. 631–658.
[14] M. Petzoldt, *A posteriori error estimators for elliptic equations with discontinuous coefficients*, Adv. Comput. Math., 16 (2002), pp. 47–75.
[15] M. Picasso, *Adaptive finite elements for a linear parabolic problem*, Comput. Methods Appl. Mech. Engrg., 167 (1998), pp. 223–237.
[16] R. Stevenson, *An optimal adaptive finite element method*, SIAM J. Numer. Anal., 42 (2005), pp. 2188–2217.
[17] R. Verfürth, *A Review of A Posteriori Error Estimation and Adaptive Mesh-Refinement Techniques*, John Wiley & Sons, Chichester-New York, 1996.
[18] R. Verfürth, *A posteriori error estimates for finite element discretization of the heat equations*, Calcolo, 40 (2003), pp. 195–212.
[19] O. C. Zienkiewicz and J. Z. Zhu, *A simple error estimator and adaptive procedure for practical engineering analysis*, Internat. J. Numer. Methods Engrg., 24 (1987), pp. 337–357.